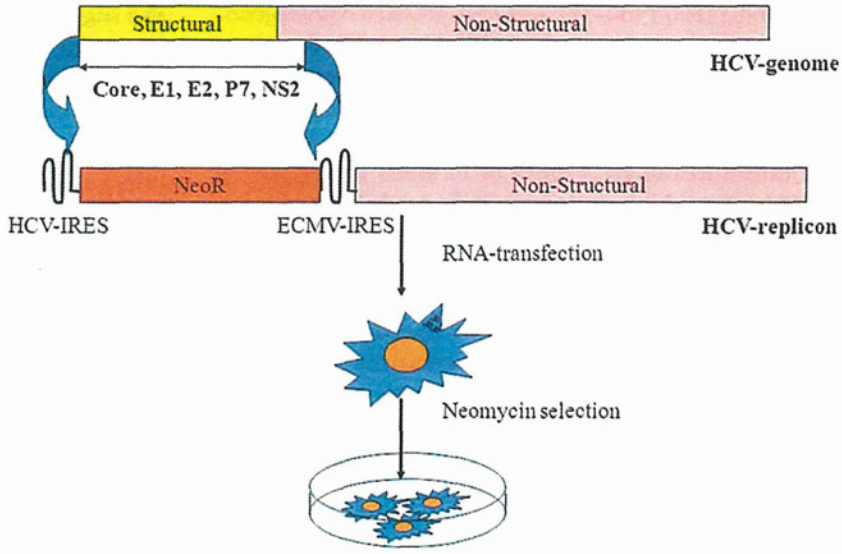

Fig. 2. HCV replicon system. The structural sequences (C, E1, E2, and p7) together with NS2 were replaced by a neomycin antibiotic-resistance gene, and an ECMV-IRES was introduced to drive translation of the remaining non-structural proteins. Neomycin selection of these double cistron (bicistronic) replicons in the hepatoma cell line Huh7 resulted in high-level HCV-RNA replication, depending on the gain of so-called 'tissue-culture' adaptive mutations mostly confined to the NS3, NS4B, and NS5A regions.

However, an apparent shortcoming of these models was that stable cell clones containing self-replicating replicons and expressing all viral proteins remained unable to release infectious HCV particles. The inability to secrete viral particles may be the consequence of adaptive mutations, which are needed to enhance viral replication rates, but at the same time may block viral assembly. Indeed, replicons without adaptive mutations show very low replication rates (16, 24). A different situation emerged when the first genotype 2a consensus genome was established (25, 26).

A subgenomic replicon constructed from a clone called JFH-1, isolated from a Japanese patient with fulminant hepatitis C, replicated up to 20-fold higher in HuH-7 cells as compared to Con1 replicons, and did not require adaptive mutations for efficient replication *in vitro* (26). Transfection of HuH-7 and HuH-7.5.1 cells with the *in vitro*-transcribed full-length JFH-1 genome or a recombinant chimeric genome with another genotype 2a isolate, J6, resulted in the secretion of viral particles that were infectious in cultured cells (Fig. 3), in chimeric mice, and in chimpanzees (27–29).

The infectivity of cells could be neutralized with antibodies against the HCV entry receptor CD81, antibodies against E2, or immunoglobulins from chronically infected patients. Importantly, the replication of cell-cultured HCV in this system was inhibited by IFN-α as well as by several HCV-specific antiviral compounds (29). Since 2005, chimeric JFH-1-based genomes have been constructed of all seven known HCV genotypes. Similar to the J6-JFH-1 chimera, in these so-called intergenotypic recombinants, the structural genes (core, E1, and E2), p7, and NS2 of JFH-1 were replaced by genotype-specific sequences which often resulted in lower infectious virion production than

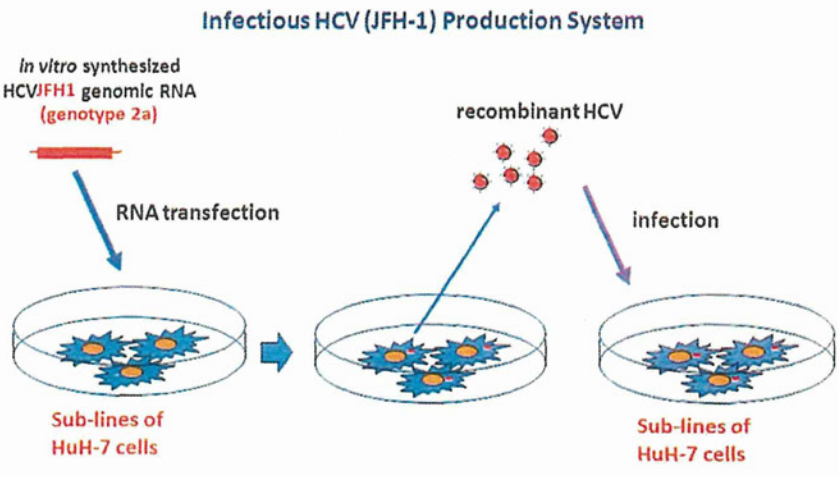

Fig. 3. JFH1 infectious system. Full-length JFH1-RNA is transcribed *in vitro*, and transfected to HuH-7-derived cell lines. JFH1 replicates in these cells, and produce infectious virions in the medium. The medium is collected, concentrated, and used to infect naive cells. Hence, the entire HCV life cycle was reproduced for the first time *in vitro*.

wild-type JFH-1 (30–32). Most NS proteins of intergenotypic chimeras originate from JFH-1, and therefore these genomes are unlikely to reflect genotype-specific characteristics of replication. However, these intergenotypic chimeras may become critically important in the study of differences in HCV entry or to assess the efficacy of HCV entry inhibitors. Interestingly, production of infectious genotype 1a HCV in cells transfected with synthetic RNA (H77-S) derived from a prototype virus (H77-C) was also reported (33). H77-S carries adaptive mutations that promote efficient viral RNA replication in HuH-7.5 cells. These mutations are located within the NS3/4A protease complex, and the NS5A protein (34) H77-S showed similar replication efficiency to JFH-1 isolate; however, it showed lower expression of HCV core protein, and lower production of infectious HCV particles (33).

Serum-derived HCV infection

The previously mentioned models used to study HCV infection are based on subclones of HuH-7 cells infected with JFH1 recombinant virus or its derivatives (27). HuH-7 cells and its subclones, however, do not support the entire life cycle of the bbHCV present in the blood of patients (35). Moreover, HCV has considerable diversity and variability. It is generally classified into six major genotypes and more than 100 subtypes (36). JFH1, however, is a single isolate of HCV genotype 2a that was originally derived from a patient with rare fulminant hepatitis (27). Thus, usage of HCV particles isolated from patient serum could be more useful to study authentic HCV infection.

Many researchers have attempted to develop an *in vitro* system for bbHCV (37–39). These current systems, however, are still insufficient due to their low efficiency for infectivity and replication of bbHCV. Normal human hepatocytes are the ideal system in which to study HCV infectivity. When cultured *in vitro*, however, they proliferate poorly and divide only a few times (40). Continuous proliferation could be achieved by introducing oncogenes, the HPV/E6E7 immortalized multiple cell types that were phenotypically and functionally similar to the parental cells (41–45). We established a human primary non-neoplastic hepatocyte cell line transduced with the HPV18/E6E7 that retained primary hepatocyte characteristics even after prolonged culture (35). We further improved the susceptibility of HPV18/E6E7-immortalized hepatocytes (HuS-E/2 cells) to bbHCV infectivity by impairing the innate immune response of these cells through suppression of interferon regulatory factor-7 (IRF-7) expression. These cells were useful to assay infectivity of HCV strains other than JFH-1, HCV replication, innate immune system engagement of HCV, and screening of anti-HCV agents. This infection system using non-neoplastic cells also suggested that IRF-7 plays an important role in eliminating HCV infection. Using this system, the suppressive effect of tamoxifen and mir199 on HCV replication was reported (46, 47).

Three-dimensional culture

A major limitation of the immortalized hepatocytes infection system was the failure to produce infectious HCV particles. Because the 3-D cell culture condition more closely reproduces the *in vivo* environment of hepatocytes (48), culturing these cells in this manner may support the entire HCV life cycle. Similarly, a previous report showed the production of HCV particles from the FLC4 hepatocyte line transfected with HCV-RNA and cultured in a 3-D radial-flow bioreactor (RFB). The RFB system is composed of a dedicated device containing 1×10^9 FLC4 cells with a culture area of 2.7 m^2. A more convenient, smaller and easy to use 3-D culture system is required for the study of the several aspects of bbHCV infection. (49). A hybrid artificial liver support system was developed using animal hepatocytes cultured in a 3-D/HF. This bioartificial liver showed several characteristic features of liver tissue for more than 4 months (50–52).

By growing our HuSE/2 cells in a similar 3-D culture (53) the gene expression profile was improved to more closely match that of human primary hepatocytes. We used this small 3-D culture system and showed it to be ideal for culturing HuS-E/2 cells for the study of bbHCV infection (Fig. 4) (54). Using this system we observed not only the enhancement of HCV replication, but also the production of infectious HCV particles in the medium using the 3-D/HF system. The cell mass formed by the 3-D culture system, most likely the polar character, was essential for the life cycle of bbHCV. Using microarray comparison of gene expression between 2-D and 3-D cultured cells, we found a higher activation of the PPAR-α signaling pathway which was shown to be important for the improvement of HCV replication in 3-D culture. Suppression of the PPAR-α signaling pathway using its antagonist MK886 markedly suppressed HCV replication in two different cell lines (53). A recent study showed that the induction of PPAR-α or PPAR-γ led to the suppression or enhancement of HCV replication, respectively, in HuH-7 cells (55). Using HuH-7-derived clones, three different independent studies confirmed our data, showing the suppression of HCV replication by PPAR-α blockers such as (MK886) (56, 57) or 2-chloro-5-nitro-*N*-(pyridyl) benzamide (BA) (58). Furthermore, no effect of PPAR-γ was observed on HCV replication (58).

Delayed production of infectious particles was also observed in cells infected with some HCV strains after prolonged culture (54). It is likely that mutation of the HCV

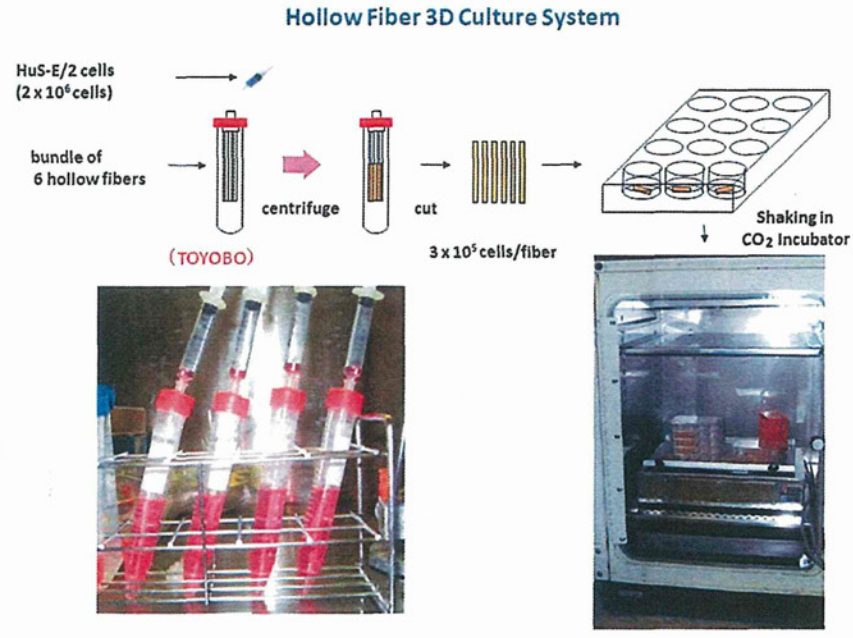

Fig. 4. 3-D hollow fiber culture. HuS-E/2 suspension was injected into the lumen of the hollow fiber system (HF; Toyobo Co., Osaka, Japan). The bundles were centrifuged to induce organoid formation. The lower 1.5 cm containing the organoid formation was then cut and cultured in 12-well plates (two capillary bundles per well) with gentle rotation using serum-free medium (Toyobo Co.) in a CO_2 incubator at 37°C. The number of cells was adjusted to 3×10^5 cells per two-capillary bundle at the start of each experiment.

genome and/or selection of clones during prolonged culture improved the productivity of infectious particles. This lack of production of infectious particles soon after infection may serve to avoid an early strong response from the host immune system, and demonstrates a novel mechanism of latent infection by HCV. Similarly, fluctuation in HCV proliferation was observed during the prolonged culture of 3-D-HuS-E/2 cells infected with bbHCV (54); this fluctuation was associated with a change in viral quasispecies, suggesting that an HCV strain having a growth advantage proliferates selectively and dominantly in these culture conditions. Because the progressive emergence of each dominant strain was only temporary, it is highly likely that the infection and proliferation of such an HCV strain is suppressed by cellular mechanism(s). Our results showed two cellular mechanisms functioning to do this. The first is the involvement of the innate immune system, as evidenced by the secretion of IFN-α during the first week of infection. The second mechanism is HCV-induced apoptosis. Although HCV-induced apoptosis was not found when HCV-1b was used for infection, it was found in all cases where HCV-2a was used, suggesting a higher cytopathic tendency of the HCV-2a genotype.

Mouse cells permissible to HCV infection

The development of prophylaxis and novel therapeutics to treat HCV infection has been hampered by the lack of suitable animal models, a deficit resulting from the limited species tropism of HCV. Chimpanzees are the only available immunocompetent *in vivo* experimental system, but their use is limited by ethical concerns, restricted availability and prohibitively high costs (59).

A convenient small-animal model supporting the HCV life cycle could significantly accelerate the preclinical testing of vaccine and drug candidates, as well as facilitate *in vivo* studies of HCV pathogenesis. A murine model was described in which overexpression of a uPA transgene resulted not only in neonatal bleeding disorders, but also in severe liver toxicity (60). Importantly, the diseased liver could be replaced by donor hepatocytes of murine origin, as well as by hepatocytes from rats, woodchucks, and humans once the uPA transgenic mice were backcrossed on an immunodeficient background. Mice with chimeric human livers that were inoculated with serum from HCV-positive donors developed prolonged HCV infections with high viral titers and evidence for active replication of the virus in chimeric human livers (61). At present, the chimeric human liver uPA/SCID mouse model is physiologically closest to a natural human infection and therefore represents the most successful small-animal model for HCV infection. Several shortcomings, however, limit its widespread use and application. Most importantly, the immunodeficiency required to allow successful xenotransplantation precludes studies on the adaptive immune response, immunopathology, and active immunization strategies (vaccine development). Second, only a few laboratories have reported successful generation of these chimeras, because this model requires high-quality human donor hepatocytes and the actual transplantation is difficult to carry out in small animals with a tendency to bleed. Finally, the efficacy of human hepatocyte engraftment is highly variable

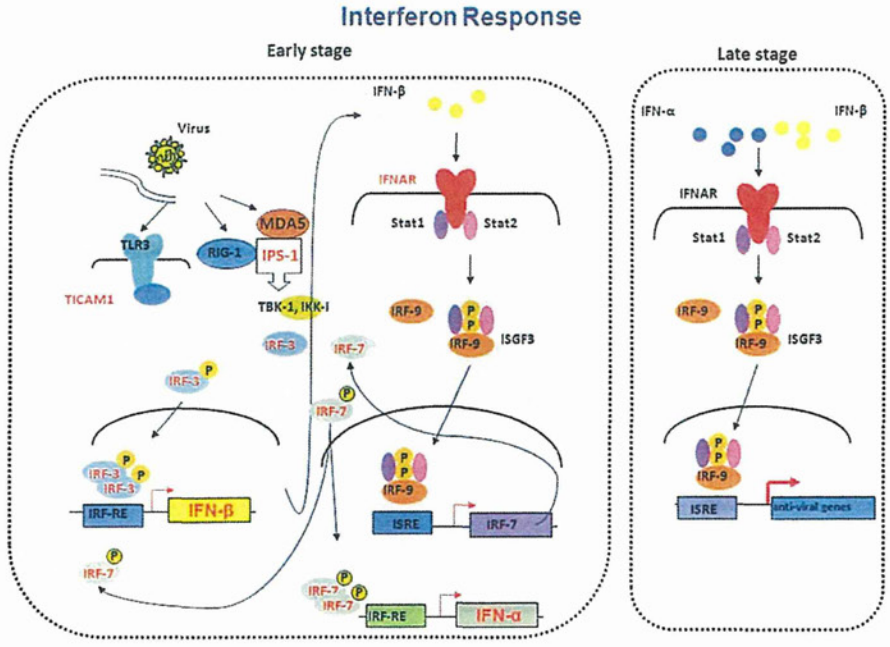

Fig. 5. Induction of interferon response by viral RNA. The cell detects viral RNA through the endosomal RNA sensor TLR3, and the cytoplasmic RNA sensors RIG-I and MDA5. Both pathways will lead to the activation of TBK-1 and IKK-I kinases, through the TICAM-1 adaptor molecule in the case of TLR3, or IPS-1 in the case of RIG-I and MDA5. These kinases will induce phosphorilization of interferon regulatory factor (IRF)-3, which will then dimerize and translocate to the nucleus. IRF-3 will then bind to the IRF response elements (IRF-RE) of IFN-β and lead to the induction of IFN-β expression. The IFN-β that is produced and secreted binds to the IFN receptor in an autocrine or paracrine manner to direct Janus Kinase Signal Transducer and Activator of Transcription (JAK-STAT) signaling and the interferon-stimulated gene factor 3 (ISGF3)-dependent expression of IRF-7 and other interferon-stimulated genes (ISG). IRF-7 will be phosphorylated by the activated TBK-1 and IKKε kinases, and form homo, or hetero-dimers with IRF-3, leading to further induction of IFN-β and -α genes. This signaling serves to amplify the IFN response by increasing the expression of IFN-β, IFN-α subtypes and ISG in a positive feedback loop.

in these animals, ranging from approximately 2% to 92% after additional treatment with an antibody to asialo- GM-1 (62).

The successful establishment of the HCV life cycle in mouse hepatocytes is another tempting alternative to overcome these problems. In addition to missing or incompatible positive regulators of HCV replication, dominant-negative restriction factors might be present in mouse hepatocytes. Altered or exacerbated innate antiviral responses, the inability of HCV proteins to overcome murine defenses, or mouse-specific restriction factors similar to those that control retroviral infection, such as Fv1, TRIM5α or APOBEC3 cytidine deaminases, could impair HCV replication in mouse cells.

In mammalian cells, the host detects and responds to infection by RNA-viruses, including HCV, by primarily recognizing viral RNA through several distinct pathogen recognition receptors (PRR), including the cell surface and endosomal RNA sensors TLR3 and TLR7, and the cytoplasmic RNA sensors RIG-I and MDA5 (Fig. 5) (63). The detection of virus infection by these receptors leads to the induction of IFN and their downstream IFN-inducible anti-viral genes through distinct signaling pathways (64). Type I IFN is an important regulator of viral infections in the innate immune system (65). Another type of IFN, IFN-lambda, affects the prognosis of HCV infection, and its response to antiviral therapy (66,67). Variations in the type or intensity of the antiviral response between hosts are known to restrict the tropism of certain viruses, such as myxoma virus, which is only permissive in mouse cells that have impaired IFN responses. Similarly, we previously reported that the impairment of IRF-7, and suppression of the interferon response improved HCV replication in immortalized primary human hepatocytes. (35)

Mutations impairing the function of the RIG-I gene and the induction of IFN were essential in establishing HCV infectivity in human HuH-7.5 cells (68). Similarly, the HCV-NS3/4a protease is known to cleave the IPS-1 adaptor molecule, inducing further downstream blocking of the IFN-inducing signaling pathway (69). These data clearly demonstrate that the host RIG-I pathway is crucial for suppressing HCV proliferation in human hepatocytes. Using a similar strategy, we investigated whether suppressing the antiviral host innate immune system conferred any advantage on HCV proliferation in mouse hepatocytes (70). We examined the possibility of HCV replication

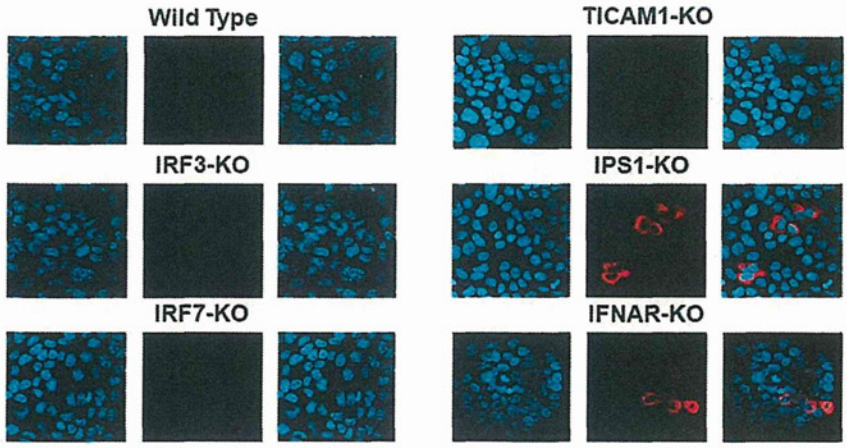

Fig. 6. Establishment of mouse hepatocyte lines permissive to J6/JFH1.
Immunofluorescence detection of J6JFH1 proteins' expression 5 days after transfection of J6JFH1-RNA through electroporation into wild-type, IRF-3-ko, IRF-7-ko, TICAM1-ko, IPS-1-ko, and IFNAR-ko, freshly isolated primary hepatocytes. A highly sensitive polyclonal antibody extracted from HCV-patient serum (AbS3) was used for the detection.

in mice lacking the expression of key factors that modulate the type I IFN-inducing pathways (Fig. 6). Only gene silencing of IFNAR or IPS-1 was sufficient to establish spontaneous HCV replication in mouse hepatocytes.

To establish a cell line permissive for HCV replication, which is required for further *in vitro* studies of the HCV life cycle in mouse hepatocytes, we immortalized IFNAR- and IPS-1-ko mice hepatocytes with SV40 T antigen. Upon expression of the human (h)CD81 gene, these newly established cell lines were able to support HCV infection and replication for the first time in mouse hepatocytes. Using these cell lines, we demonstrated that the suppression of IPS-1 enhances HCV infection and replication in mouse hepatocytes through the suppression of both IFN induction and an IFN-independent J6JFH1-induced cytopathic effect. We also showed for the first time the importance of the HCV structural region for viral replication, as JFH1 chimera containing the J6 structure region showed a privilege for spontaneous replication over full-length JFH1 or the subgenomic JFH1 replicon. IRF-3-ko MEF were previously shown to support HCV replication more efficiently than wild MEF (71). As the knockout of IPS-1 mainly suppresses signaling in response to virus RNA detection, and maintains an intact IFN response and induction to other stimulants, it may result in minimum interference to adaptive immune responses as compared to IRF-3 or IFNAR-ko.

Conclusion

We have established an *in vitro* culture system that can support the entire life cycle of a variety of HCV isolates and genotypes. Although this *in vitro* model system may not completely reproduce the *in vivo* situation, we believe it is the first *in vitro* system showing HCV strain-dependent virus/cell interaction including induction of cellular apoptosis and/or evasion from the cellular innate immune response, which may make it a good tool for the analysis of virus/host interaction, together with the development of new anti-HCV strategies for the different bbHCV strains. We have also established hepatocyte lines from IPS-1-ko mice that support HCV replication and infection. These cell lines will be very useful in identifying other species' restriction factors and viral determinants required for the further establishment of a robust and efficient HCV life cycle in mouse hepatocytes. Further development of hCD81-transgenic IPS-1-ko mice may serve as a good model for the study of immunological responses against HCV infection. This mouse model can be used as a backbone for any further future models supporting robust HCV infectivity for the study of HCV pathogenesis, propagation and vaccine development.

ACKNOWLEDGMENT

The author wish to thank Dr. Jin Takahashi from the Japanese NIH, NIID for his help designing figure 5 in this paper.

DISCLOSURE

The authors declare no financial or commercial conflict of interest.

REFERENCES

1. Seto W.K., Lai C.L., Fung J., Hung I., Yuen J., Young J., Wong D.K., Yuen M.F. (2010) Natural history of chronic hepatitis C: Genotype 1 versus genotype 6. *J Hepatol.*
2. Conry-Cantilena C., Vanraden M., Gibble J., Melpolder J., Shakil A.O., Viladomiu L., Cheung L., Dibisceglie A., Hoofnagle J., Shih J.W., Kaslow R., Ness P., Alter H.J. (1996) Routes of infection, viremia, and liver disease in blood donors found to have hepatitis C virus infection. *N Engl J Med* **334**: 1691–6.
3. Alter M.J., Kruszon-Moran D., Nainan O.V., Mcquillan G.M., Gao F., Moyer L.A., Kaslow R.A., Margolis H.S. (1999) The prevalence of hepatitis C virus infection in the United States, 1988 through 1994. *N Engl J Med* **341**: 556–62.
4. Brown R.S. (2005) Hepatitis C and liver transplantation. *Nature* **436**: 973–8.

5. Shepard C.W., Finelli L., Alter M.J. (2005) Global epidemiology of hepatitis C virus infection. *Lancet Infect Dis* **5**: 558–67.
6. Penin F., Dubuisson J., Rey F.A., Moradpour D., Pawlotsky J.M. (2004) Structural biology of hepatitis C virus. *Hepatology* **39**: 5–19.
7. Moradpour D., Penin F., Rice C.M. (2007) Replication of hepatitis C virus. *Nat Rev Microbiol* **5**: 453–63.
8. Bartenschlager R., Lohmann V. (2000) Replication of hepatitis C virus. *J Gen Virol* **81**: 1631–48.
9. El-Farrash M.A., Aly H.H., Watashi K., Hijikata M., Egawa H., Shimotohno K. (2007) In vitro infection of immortalized primary hepatocytes by HCV genotype 4a and inhibition of virus replication by cyclosporin. *Microbiol Immunol* **51**: 127–33.
10. Lohmann V., Korner F., Koch J., Herian U., Theilmann L., Bartenschlager R. (1999) Replication of subgenomic hepatitis C virus RNAs in a hepatoma cell line. *Science* **285**: 110–3.
11. Pietschmann T., Lohmann V., Rutter G., Kurpanek K., Bartenschlager R. (2001) Characterization of cell lines carrying self-replicating hepatitis C virus RNAs. *J Virol* **75**: 1252–64.
12. Windisch M.P., Frese M., Kaul A., Trippler M., Lohmann V., Bartenschlager R. (2005) Dissecting the interferon-induced inhibition of hepatitis C virus replication by using a novel host cell line. *J Virol* **79**: 13778–93.
13. Date T., Kato T., Miyamoto M., Zhao Z., Yasui K., Mizokami M., Wakita T. (2004) Genotype 2a hepatitis C virus subgenomic replicon can replicate in HepG2 and IMY-N9 cells. *J Biol Chem* **279**: 22371–6.
14. Kato N., Mori K., Abe K., Dansako H., Kuroki M., Ariumi Y., Wakita T., Ikeda M. (2009) Efficient replication systems for hepatitis C virus using a new human hepatoma cell line. *Virus Res* **146**: 41–50.
15. Ali S., Pellerin C., Lamarre D., Kukolj G. (2004) Hepatitis C virus subgenomic replicons in the human embryonic kidney 293 cell line. *J Virol* **78**: 491–501.
16. Blight K.J., Mckeating J.A., Rice C.M. (2002) Highly permissive cell lines for subgenomic and genomic hepatitis C virus RNA replication. *J Virol* **76**: 13001–14.
17. Friebe P., Boudet J., Simorre J.P., Bartenschlager R. (2005) Kissing-loop interaction in the 3' end of the hepatitis C virus genome essential for RNA replication. *J Virol* **79**: 380–92.
18. Lohmann V., Korner F., Dobierzewska A., Bartenschlager R. (2001) Mutations in hepatitis C virus RNAs conferring cell culture adaptation. *J Virol* **75**: 1437–49.
19. Lohmann V., Hoffmann S., Herian U., Penin F., Bartenschlager R. (2003) Viral and cellular determinants of hepatitis C virus RNA replication in cell culture. *J Virol* **77**: 3007–19.
20. Krieger N., Lohmann V., Bartenschlager R. (2001) Enhancement of hepatitis C virus RNA replication by cell culture-adaptive mutations. *J Virol* **75**: 4614–24.
21. Blight K.J., Mckeating J.A., Marcotrigiano J., Rice C.M. (2003) Efficient replication of hepatitis C virus genotype 1a RNAs in cell culture. *J Virol* **77**: 3181–90.
22. Blight K.J., Kolykhalov A.A., Rice C.M. (2000) Efficient initiation of HCV RNA replication in cell culture. *Science* **290**: 1972–4.
23. Bartenschlager R. (2005) The hepatitis C virus replicon system: from basic research to clinical application. *J Hepatol* **43**: 210–6.
24. Pietschmann T., Lohmann V., Kaul A., Krieger N., Rinck G., Rutter G., Strand D., Bartenschlager R. (2002) Persistent and transient replication of full-length hepatitis C virus genomes in cell culture. *J Virol* **76**: 4008–21.
25. Kato T., Furusaka A., Miyamoto M., Date T., Yasui K., Hiramoto J., Nagayama K., Tanaka T., Wakita T. (2001) Sequence analysis of hepatitis C virus isolated from a fulminant hepatitis patient. *J Med Virol* **64**: 334–9.
26. Kato T., Date T., Miyamoto M., Furusaka A., Tokushige K., Mizokami M., Wakita T. (2003) Efficient replication of the genotype 2a hepatitis C virus subgenomic replicon. *Gastroenterology* **125**: 1808–17.
27. Wakita T., Pietschmann T., Kato T., Date T., Miyamoto M., Zhao Z., Murthy K., Habermann A., Krausslich H.G., Mizokami M., Bartenschlager R., Liang T.J. (2005) Production of infectious hepatitis C virus in tissue culture from a cloned viral genome. *Nat Med* **11**: 791–6.
28. Zhong J., Gastaminza P., Cheng G., Kapadia S., Kato T., Burton D.R., Wieland S.F., Uprichard S.L., Wakita T., Chisari F.V. (2005) Robust hepatitis C virus infection in vitro. *Proc Natl Acad Sci U S A* **102**: 9294–9.
29. Lindenbach B.D., Evans M.J., Syder A.J., Wolk B., Tellinghuisen T.L., Liu C.C., Maruyama T., Hynes R.O., Burton D.R., Mckeating J.A., Rice C.M. (2005) Complete replication of hepatitis C virus in cell culture. *Science* **309**: 623–6.
30. Yi M., Ma Y., Yates J., Lemon S.M. (2007) Compensatory mutations in E1, p7, NS2, and NS3 enhance yields of cell culture-infectious intergenotypic chimeric hepatitis C virus. *J Virol* **81**: 629–38.
31. Pietschmann T., Kaul A., Koutsoudakis G., Shavinskaya A., Kallis S., Steinmann E., Abid K., Negro F., Dreux M., Cosset F.L., Bartenschlager R. (2006) Construction and characterization of infectious intragenotypic and intergenotypic hepatitis C virus chimeras. *Proc Natl Acad Sci U S A* **103**: 7408–13.
32. Gottwein J.M., Scheel T.K., Jensen T.B., Lademann J.B., Prentoe J.C., Knudsen M.L., Hoegh A.M., Bukh J. (2009) Development and characterization of hepatitis C virus genotype 1-7 cell culture systems: role of CD81 and scavenger receptor class B type I and effect of antiviral drugs. *Hepatology* **49**: 364–77.
33. Yi M., Villanueva R.A., Thomas D.L., Wakita T., Lemon S.M. (2006) Production of infectious genotype 1a hepatitis C virus (Hutchinson strain) in cultured human hepatoma cells. *Proc Natl Acad Sci U S A* **103**: 2310–5.
34. Yi M., Lemon S.M. (2004) Adaptive mutations producing efficient replication of genotype 1a hepatitis C virus RNA in normal Huh7 cells. *J Virol* **78**: 7904–15.
35. Aly H.H., Watashi K., Hijikata M., Kaneko H., Takada Y., Egawa H., Uemoto S., Shimotohno K. (2007) Serum-derived hepatitis C virus infectivity in interferon regulatory factor-7-suppressed human primary hepatocytes. *J Hepatol* **46**: 26–36.
36. Forns X., Bukh J. (1999) The molecular biology of hepatitis C virus. Genotypes and quasispecies. *Clin Liver Dis* **3**: 693–716, vii.
37. Ikeda M., Sugiyama K., Mizutani T., Tanaka T., Tanaka K., Sekihara H., Shimotohno K., Kato N. (1998) Human hepatocyte clonal cell lines that support persistent replication of hepatitis C virus. *Virus Res* **56**: 157–67.
38. Chong T.W., Smith R.L., Hughes M.G., Camden J., Rudy C.K., Evans H.L., Sawyer R.G., Pruett T.L. (2006) Primary human hepatocytes in spheroid formation to study hepatitis C infection. *J Surg Res* **130**: 52–7.
39. Molina S., Castet V., Pichard-Garcia L., Wychowski C., Meurs E., Pascussi J.M., Sureau C., Fabre J.M., Sacunha A., Larrey D., Dubuisson J., Coste J., Mckeating J., Maurel P., Fournier-Wirth C. (2008) Serum-derived hepatitis C virus infection of primary human hepatocytes is tetraspanin CD81 dependent. *J Virol* **82**: 569–74.
40. Delgado J.P., Parouchev A., Allain J.E., Pennarun G., Gauthier L.R., Dutrillaux A.M., Dutrillaux B., Di Santo J., Capron F., Boussin F.D., Weber A. (2005) Long-term controlled immortalization of a primate hepatic progenitor cell line after Simian virus 40 T-Antigen gene transfer. *Oncogene* **24**: 541–51.
41. Chen W.H., Lai W.F., Deng W.P., Yang W.K., Lo W.C., Wu C.C., Yang D.M., Lai M.T., Lin C.T., Lin T.W., Yang C.B. (2006) Tissue

engineered cartilage using human articular chondrocytes immortalized by HPV-16 E6 and E7 genes. *J Biomed Mater Res A* **76**: 512–20.
42. Dimri G., Band H., Band V. (2005) Mammary epithelial cell transformation: insights from cell culture and mouse models. *Breast Cancer Res* **7**: 171–9.
43. Harms W., Rothamel T., Miller K., Harste G., Grassmann M., Heim A. (2001) Characterization of human myocardial fibroblasts immortalized by HPV16 E6–E7 genes. *Exp Cell Res* **268**: 252–61.
44. Shiga T., Shirasawa H., Shimizu K., Dezawa M., Masuda Y., Simizu B. (1997) Normal human fibroblasts immortalized by introduction of human papillomavirus type 16 (HPV-16) E6-E7 genes. *Microbiol Immunol* **41**: 313–9.
45. Akimov S.S., Ramezani A., Hawley T.S., Hawley R.G. (2005) Bypass of senescence, immortalization, and transformation of human hematopoietic progenitor cells. *Stem Cells* **23**: 1423–33.
46. Watashi K., Inoue D., Hijikata M., Goto K., Aly H.H., Shimotohno K. (2007) Anti-hepatitis C virus activity of tamoxifen reveals the functional association of estrogen receptor with viral RNA polymerase NS5B. *J Biol Chem* **282**: 32765–72.
47. Murakami Y., Aly H.H., Tajima A., Inoue I., Shimotohno K. (2009) Regulation of the hepatitis C virus genome replication by miR-199a. *J Hepatol* **50**: 453–60.
48. Andrei G. (2006) Three-dimensional culture models for human viral diseases and antiviral drug development. *Antiviral Res* **71**: 96–107.
49. Aizaki H., Nagamori S., Matsuda M., Kawakami H., Hashimoto O., Ishiko H., Kawada M., Matsuura T., Hasumura S., Matsuura Y., Suzuki T., Miyamura T. (2003) Production and release of infectious hepatitis C virus from human liver cell cultures in the three-dimensional radial-flow bioreactor. *Virology* **314**: 16–25.
50. Mizumoto H., Ishihara K., Nakazawa K., Ijima H., Funatsu K., Kajiwara T. (2008) A new culture technique for hepatocyte organoid formation and long-term maintenance of liver-specific functions. *Tissue Eng Part C Methods* **14**: 167–75.
51. Funatsu K., Ijima H., Nakazawa K., Yamashita Y., Shimada M., Sugimachi K. (2001) Hybrid artificial liver using hepatocyte organoid culture. *Artif Organs* **25**: 194–200.
52. Mizumoto H., Aoki K., Nakazawa K., Ijima H., Funatsu K., Kajiwara T. (2008) Hepatic differentiation of embryonic stem cells in HF/organoid culture. *Transplant Proc* **40**: 611–3.
53. Aly H.H., Shimotohno K., Hijikata M. (2009) 3D cultured immortalized human hepatocytes useful to develop drugs for blood-borne HCV. *Biochem Biophys Res Commun* **379**: 330–4.
54. Aly H.H., Qi Y., Atsuzawa K., Usuda N., Takada Y., Mizokami M., Shimotohno K., Hijikata M. (2009) Strain-dependent viral dynamics and virus-cell interactions in a novel in vitro system supporting the life cycle of blood-borne hepatitis C virus. *Hepatology* **50**: 689–96.
55. Nishimura-Sakurai Y., Sakamoto N., Mogushi K., Nagaie S., Nakagawa M., Itsui Y., Tasaka-Fujita M., Onuki-Karakama Y., Suda G., Mishima K., Yamamoto M., Ueyama M., Funaoka Y., Watanabe T., Azuma S., Sekine-Osajima Y., Kakinuma S., Tsuchiya K., Enomoto N., Tanaka H., Watanabe M. (2010) Comparison of HCV-associated gene expression and cell signaling pathways in cells with or without HCV replicon and in replicon-cured cells. *J Gastroenterol* **45**: 523–36.
56. Chockalingam K., Simeon R.L., Rice C.M., Chen Z. (2010) A cell protection screen reveals potent inhibitors of multiple stages of the hepatitis C virus life cycle. *Proc Natl Acad Sci U S A* **107**: 3764–9.
57. Gastaminza P., Whitten-Bauer C., Chisari F.V. (2010) Unbiased probing of the entire hepatitis C virus life cycle identifies clinical compounds that target multiple aspects of the infection. *Proc Natl Acad Sci U S A* **107**: 291–6.
58. Rakic B., Sagan S.M., Noestheden M., Belanger S., Nan X., Evans C.L., Xie X.S., Pezacki J.P. (2006) Peroxisome proliferator-activated receptor alpha antagonism inhibits hepatitis C virus replication. *Chem Biol* **13**: 23–30.
59. Bukh J. (2004) A critical role for the chimpanzee model in the study of hepatitis C. *Hepatology* **39**: 1469–75.
60. Heckel J.L., Sandgren E.P., Degen J.L., Palmiter R.D., Brinster R.L. (1990) Neonatal bleeding in transgenic mice expressing urokinase-type plasminogen activator. *Cell* **62**: 447–56.
61. Mercer D.F., Schiller D.E., Elliott J.F., Douglas D.N., Hao C., Rinfret A., Addison W.R., Fischer K.P., Churchill T.A., Lakey J.R., Tyrrell D.L., Kneteman N.M. (2001) Hepatitis C virus replication in mice with chimeric human livers. *Nat Med* **7**: 927–33.
62. Tateno C., Yoshizane Y., Saito N., Kataoka M., Utoh R., Yamasaki C., Tachibana A., Soeno Y., Asahina K., Hino H., Asahara T., Yokoi T., Furukawa T., Yoshizato K. (2004) Near completely humanized liver in mice shows human-type metabolic responses to drugs. *Am J Pathol* **165**: 901–12.
63. Diamond M.S. (2009) Mechanisms of evasion of the type I interferon antiviral response by flaviviruses. *J Interferon Cytokine Res* **29**: 521–30.
64. O'neill L.A., Bowie A.G. (2010) Sensing and signaling in antiviral innate immunity. *Curr Biol* **20**: R328–33.
65. Platanias L.C. (2005) Mechanisms of type-I- and type-II-interferon-mediated signalling. *Nat Rev Immunol* **5**: 375–86.
66. Tanaka Y., Nishida N., Sugiyama M., Kurosaki M., Matsuura K., Sakamoto N., Nakagawa M., Korenaga M., Hino K., Hige S., Ito Y., Mita E., Tanaka E., Mochida S., Murawaki Y., Honda M., Sakai A., Hiasa Y., Nishiguchi S., Koike A., Sakaida I., Imamura M., Ito K., Yano K., Masaki N., Sugauchi F., Izumi N., Tokunaga K., Mizokami M. (2009) Genome-wide association of IL28B with response to pegylated interferon-alpha and ribavirin therapy for chronic hepatitis C. *Nat Genet* **41**: 1105–9.
67. Thompson A.J., Muir A.J., Sulkowski M.S., Ge D., Fellay J., Shianna K.V., Urban T., Afdhal N.H., Jacobson I.M., Esteban R., Poordad F., Lawitz E.J., Mccone J., Shiffman M.L., Galler G.W., Lee W.M., Reindollar R., King J.W., Kwo P.Y., Ghalib R.H., Freilich B., Nyberg L.M., Zeuzem S., Poynard T., Vock D.M., Pieper K.S., Patel K., Tillmann H.L., Noviello S., Koury K., Pedicone L.D., Brass C.A., Albrecht J.K., Goldstein D.B., Mchutchison J.G. (2010) Interleukin-28B polymorphism improves viral kinetics and is the strongest pretreatment predictor of sustained virologic response in genotype 1 hepatitis C virus. *Gastroenterology* **139**: 120–9 e18.
68. Sumpter R., Jr., Loo Y.M. Foy E., Li K., Yoneyama M., Fujita T., Lemon S.M., Gale M., Jr. (2005) Regulating intracellular antiviral defense and permissiveness to hepatitis C virus RNA replication through a cellular RNA helicase, RIG-I. *J Virol* **79**: 2689–99.
69. Foy E., Li K., Sumpter R., Jr., Loo Y.M., Johnson C.L., Wang C., Fish P.M., Yoneyama M., Fujita T., Lemon S.M., Gale M., Jr. (2005) Control of antiviral defenses through hepatitis C virus disruption of retinoic acid-inducible gene-I signaling. *Proc Natl Acad Sci U S A* **102**: 2986–91.
70. Aly H.H., Oshiumi H., Shime H., Matsumoto M., Wakita T., Shimotohno K., Seya T. (2011) Development of mouse hepatocyte lines permissive for hepatitis C virus (HCV). *PLoS One* **6**: e21284.
71. Lin L.T., Noyce R.S., Pham T.N., Wilson J.A., Sisson G.R., Michalak T.I., Mossman K.L., Richardson C.D. (2010) Replication of subgenomic hepatitis C virus replicons in mouse fibroblasts is facilitated by deletion of interferon regulatory factor 3 and expression of liver-specific microRNA 122. *J Virol* **84**: 9170–80.

OPEN ACCESS Freely available online

PLOS | ONE

Dendritic Cells from Oral Cavity Induce Foxp3$^+$ Regulatory T Cells upon Antigen Stimulation

Sayuri Yamazaki[1,2*☯], Akira Maruyama[1☯], Kohei Okada[1], Misako Matsumoto[1], Akimichi Morita[2], Tsukasa Seya[1*]

1 Department of Microbiology and Immunology, Graduate School of Medicine, Hokkaido University, Sapporo, Japan, **2** Department of Geriatric and Environmental Dermatology, Nagoya City University, Graduate School of Medical Sciences, Nagoya, Japan

Abstract

Evidence is accumulating that dendritic cells (DCs) from the intestines have the capacity to induce Foxp3$^+$CD4$^+$ regulatory T cells (T-regs) and regulate immunity versus tolerance in the intestines. However, the contribution of DCs to controlling immunity versus tolerance in the oral cavity has not been addressed. Here, we report that DCs from the oral cavity induce Foxp3$^+$ T-regs as well as DCs from intestine. We found that oral-cavity-draining cervical lymph nodes contained higher frequencies of Foxp3$^+$ T-regs and ROR-γt$^+$ CD4$^+$T cells than other lymph nodes. The high frequency of Foxp3$^+$ T-regs in the oral-cavity-draining cervical lymph nodes was not dependent on the Toll like receptor (TLR) adaptor molecules, Myd88 and TICAM-1 (TRIF). In contrast, the high frequency of ROR-γt$^+$ CD4$^+$T cells relies on Myd88 and TICAM-1. *In vitro* data showed that CD11c$^+$ DCs from oral-cavity-draining cervical lymph nodes have the capacity to induce Foxp3$^+$ T-regs in the presence of antigen. These data suggest that, as well as in the intestinal environment, antigen-presenting DCs may play a vital role in maintaining tolerance by inducing Foxp3$^+$ T-regs in the oral cavity.

Citation: Yamazaki S, Maruyama A, Okada K, Matsumoto M, Morita A, et al. (2012) Dendritic Cells from Oral Cavity Induce Foxp3$^+$ Regulatory T Cells upon Antigen Stimulation. PLoS ONE 7(12): e51665. doi:10.1371/journal.pone.0051665

Editor: *Gourapura J Renukaradhya, The Ohio State University, United States of America*

Received August 22, 2012; **Accepted** November 6, 2012; **Published** December 18, 2012

Funding: This work was funded by a Grant-in-Aid for challenging Exploratory Research (SY) and a Grant-in-Aid for Scientific Research B (SY) from Japan Society for the Promotion of Science, the Mochida Memorial Foundation for Medical and Pharmaceutical Research (SY) and Grants-in-Aid from the Ministry of Education, Science, and Culture (Specified Project for Advanced Research) and the Ministry of Health, Labor, and Welfare of Japan. Specified financial supports by a MEXT Grant-in-Project 'the Carcinogenic Spiral' and the Japan Initiative for Global Research Network on Infectious Diseases (J-GRID) are gratefully acknowledged. These funding bodies had no role in study design, data collection or analysis, the decision to publish, or preparation of the manuscript.

Competing Interests: The authors have declared that no competing interests exist.

* E-mail: seya-tu@pop.med.hokudai.ac.jp (TS); yamazas@med.nagoya-cu.ac.jp (SY)

☯ These authors contributed equally to this work.

Introduction

Foxp3$^+$CD25$^+$CD4$^+$ regulatory T cells (T-regs), constitute about 5–10% of peripheral CD4$^+$T cells and control immunological self-tolerance in rodents and human [1,2,3,4]. The expansion and induction of CD25$^+$Foxp3$^+$ T-regs in the periphery are controlled by professional antigen-presenting cells, dendritic cells (DCs) [5,6]. DCs can expand thymic-derived natural occurring T-regs [7,8,9]. DCs are the most efficient antigen presenting cells to induce Foxp3$^+$T-regs from Foxp3$^-$ precursors in the periphery [10,11]. Peripheral DCs directly control the numbers and homeostasis of Foxp3$^+$T-regs *in vivo* [12].

Foxp3$^+$T-regs induced by DCs in the intestine control the balance between inflammation and tolerance in the gut [13,14,15]. CD103$^+$DCs in the intestine use the retinoic acid-metabolizing enzyme retinaldehyde dehydrogenase and induce Foxp3$^+$T-regs to maintain oral tolerance [16,17]. Intestinal DCs use signaling through ß-catenin to induce Foxp3$^+$T-regs, which suppress Th17 and Th1 responses in the intestine [18]. Specific pathogens or Toll-like receptor (TLR) signals have been shown to induce Foxp3$^+$T-regs in the intestine [19,20]. Moreover, Foxp3$^+$T-regs control Th17 cells using interleukin (IL)-10 in the intestine [21,22]. Thus, Foxp3$^+$T-regs in the intestine are important in maintaining mucosal tolerance where there are vast numbers of commensal microbes and food antigens.

As in the intestine, many commensal microbes and food antigens also exist in the oral cavity [23,24,25,26]. Oral cavity is often involved with systemic immunological diseases such as graft versus host diseases, Stevens-Johnson syndrome, Behçet diseases, pemphigus vulgaris and Sjögren's syndrome. In addition, oral cavity is the place where many viruses, including influenza, herpes, common cold etc., start to infect. Therefore, it is important to identify how immune response is regulated in the oral cavity. Here we found that the DCs from oral cavity have the capacity to induce Foxp3$^+$T-regs. To our knowledge, this is the first report showing that DCs from the oral cavity induce Foxp3$^+$T-regs to maintain tolerance.

Results

The Frequency of Foxp3$^+$T-regs is Increased in Cervical Lymph Nodes (CLNs) in a Myd88/TICAM-1- Independent Manner

We considered whether Foxp3$^+$T-regs played an important role in the skin or oral cavity because the skin and oral cavity are exposed to many commensal microbes and antigens, like the intestine. First, we investigated the frequencies of Foxp3$^+$T-regs in lymph nodes (LNs) at different anatomical locations, which included skin- and oral-cavity-draining LNs. We found that

cervical LNs (CLNs) contained a higher frequency of Foxp3$^+$ T-regs than other skin-draining LNs, such as axillary LNs (ALNs) and inguinal LNs (ILNs; paired t-test: $p<0.005$; Fig.1A arrow, Fig.1B and Fig.S1). CLNs contained a slightly, but significantly, higher frequency of Foxp3$^+$ T-regs than mesenteric LNs (MLNs; paired t-test $p<0.05$; Fig.1B). In MLNs, Foxp3$^+$T-regs are actively induced by CD103$^+$ DCs [16,17]. These data suggest that Foxp3$^+$T-regs may be also induced in CLNs, as in MLNs.

To investigate if the frequency of DCs correlates with the frequency of Foxp3$^+$T-regs, the frequency of CD11c$^+$DCs in total cells was compared between CLNs and ALNs (Fig.S2). The frequency of DCs was similar between CLNs and ALNs.

Recent reports showed that signals though TLR-2 induce Foxp3$^+$T-regs [20,27,28]. To examine whether signals from TLRs are required for the high frequency of Foxp3$^+$ T-regs in CLNs, we took advantage of Myd88 and TICAM-1 (TRIF) double knockout mice (Myd88/TICAM1 DKO), which lack all TLR signaling [29,30]. In Myd88/TICAM1 DKO mice, CLNs still contained a significantly higher frequency of Foxp3$^+$T-regs than inguinal LNs (ILNs; paired t-test: $p<0.05$; Fig.1B). The frequency of Foxp3$^+$T-regs in CLNs did not differ between Myd88/TICAM1 DKO and wild-type (WT) mice (t-test: $p = 0.09$; Fig.1B, 1C). The frequency of Foxp3$^+$T-regs in MLNs did not differ between Myd88/TICAM1 DKO and WT mice also (t-test: $p = 0.4$; Fig.1B).

Thus, Foxp3$^+$T-regs are increased in CLNs in a Myd88/TICAM1-independent manner, suggesting that TLR signals are not involved in the increase in Foxp3$^+$ T-regs in CLNs.

The Frequency of ROR-γt$^+$ CD4$^+$T Cells is Increased in CLNs in a Myd88/TICAM1- Dependent Manner

The induction of Foxp3$^+$T-regs in the intestine is reciprocally controlled by Th17 [18,31]. To examine the balance between Th17 and Foxp3$^+$T-regs, we next compared the frequencies of ROR-γt$^+$ CD4$^+$T cells in different anatomical locations. ROR-γt is a transcription factor expressed by Th17 cells [32]. We found that CLNs had a significantly higher frequency of ROR-γt$^+$ CD4$^+$T cells than other skin-draining LNs and spleen (paired t-test: $p<0.05$; Fig.2A closed arrows and Fig.2B). As expected, MLNs contained a higher frequency of ROR-γt$^+$ CD4$^+$T cells than other LNs (Fig.2A gray arrows and Fig.2B).

To assess whether signals from microbes through TLRs are required for the induction of ROR-γt$^+$ CD4$^+$T cells in CLNs, we investigated Myd88/TICAM1 DKO mice. In Myd88/TICAM1 DKO mice, frequencies of ROR-γt$^+$ CD4$^+$T cells did not differ between CLNs and ILNs (paired t-test: $p = 0.05$; Fig.2B). Moreover, the frequency of ROR-γt$^+$ CD4$^+$T cells in CLNs was significantly reduced in Myd88/TICAM-1 DKO mice (t-test: $p<0.05$; Fig.2B). The frequency of ROR-γt$^+$ CD4$^+$T cells in MLNs did not differ between Myd88/TICAM1 DKO and WT mice also (t-test: $p = 0.1$; Fig.2B).

Thus, both Foxp3$^+$T-regs and Th17 may be induced in CLNs. However, Myd88/TICAM1 signaling is important for the development of ROR-γt$^+$CD4$^+$-Th17 T cells in CLNs (Fig.2B), but not for the induction of Foxp3$^+$T-regs (Fig.1B).

CLNs are Oral-cavity-draining Lymph Nodes

We considered that the higher frequency of Foxp3$^+$T-regs in CLNs may reflect their response to antigens in the oral cavity. To confirm whether CLNs were draining LNs from the oral cavity, we investigated the proliferation of transferred OT-II CD4$^+$-T cells in CLNs after sublingual (s.l.) administration of ovalbumin (OVA; Fig.3). OT-II mice are commonly used OVA-specific CD4$^+$ T-cell receptor transgenic mice [7,10,28]. In the absence of OVA s.l. administration, carboxyfluorescein diacetate succinimidyl ester (CFSE)-labeled OT-II T cells did not divide, in CLNs or ALNs (Fig.3, top). With OVA s.l. administration, CFSE-labeled OT II T cells divided well in CLNs (Fig.3, bottom arrow), but not in ALNs. Thus, we confirmed that CLNs were draining LNs of the oral cavity because s.l.-administered OVA antigen was presented to OT II CD4$^+$-T cells.

DCs from Oral-cavity-draining CLNs Locate Close to Foxp3$^+$T-regs and have the Capacity to Induce Foxp3$^+$ T-regs on Antigen Stimulation

Next, to investigate the interaction between DCs and Foxp3$^+$T-regs in CLNs, we microscopically examined CLNs. We found that Foxp3$^+$T-regs and CD11c$^+$ DCs were closely located, as reported previously in MLNs [33] (Fig.4A). This suggests that DCs from CLNs may induce Foxp3$^+$T-regs as DCs do in MLNs.

To determine whether DCs from the oral cavity can in fact induce Foxp3$^+$T-regs, we compared the capacity to induce Foxp3$^+$T-regs *in vitro* using DCs from ALNs, MLNs, and oral-cavity-draining CLNs. Purified CD11c$^+$ DCs from CLNs, ALNs, or MLNs were cultured with OT II CD4$^+$T cells with or without antigen for 5 days. In the presence of antigen, CLN DCs induced a higher frequency of Foxp3$^+$T-regs compared with ALN DCs (paired t-test: $p<0.005$; Fig.4B, 4C). The frequency of Foxp3$^+$T-regs induced by antigen plus DCs did not differ between the culture with CLN DCs and that with MLN DCs (paired t-test: $p = 0.878$; Fig.4C).

These results indicated that DCs from the oral-cavity-draining CLNs had the capacity to induce Foxp3$^+$T-regs with antigen, as DCs from MLNs do.

CD103$^+$DCs may not be Involved in Inducing Foxp3$^+$ T-regs in Oral-cavity-draining CLNs

To determine whether DCs from the oral cavity contain a specific DC subset to induce Foxp3$^+$T-regs as in the intestine, we first performed real-time PCR. When we investigated the mRNA expression of retinal dehydrogenase 2 (RALDH2), transforming growth factor (TGF)-ß, and IL-10, there was no difference between DCs from CLNs and ALNs (Fig.4A). DCs from MLNs had higher mRNA expression of RALDH2 as previously reported (Fig.5A). We also measured the protein production of TGF-ß1 and IL-10 in the culture supernatant. TGF-ß1 was not detected in the culture supernatants of CLN DCs with or without latent TGF-ß activation (data not shown). We did not detect IL-10 in the culture supernatants from CLN DCs and OT II CD4$^+$T cells without peptide in Fig.4B and 4C (data not shown). Theses results indicate that TGF-ß1, IL-10 and RALDH2 may not involve in the induction of Foxp3$^+$T-regs by CLN DCs.

To investigate whether CD103$^+$DCs play a role in inducing Foxp3$^+$T-regs in CLNs, we compared the frequency of CD103$^+$DCs in each location. However, oral cavity-draining CLNs had a lower frequency of CD103$^+$ DCs than MLNs (Fig.5B).

Plasmacytoid DCs have a capacity to induce Foxp3$^+$T-regs [34,35,36,37]. Epidermal Langerhans cells and migratory dermal DCs have also been reported to induce Foxp3$^+$T-regs [38,39,40]. However, the frequencies of plasmacytoid DCs and migratory class II^{high} DCs did not differ between CLNs and ALNs (Fig.5C). Next, we investigated the classical CD8$^+$ and CD8$^-$ DC subsets in CLNs and ALNs. The frequency of CD8$^+$ DCs was similar between CLNs and ALNs (paired t test: $p = 0.065$) (Fig.5D). However, CLNs had a significantly higher frequency of CD8$^-$ DCs than ALNs (paired t test: $p<0.0005$) (Fig.5D).

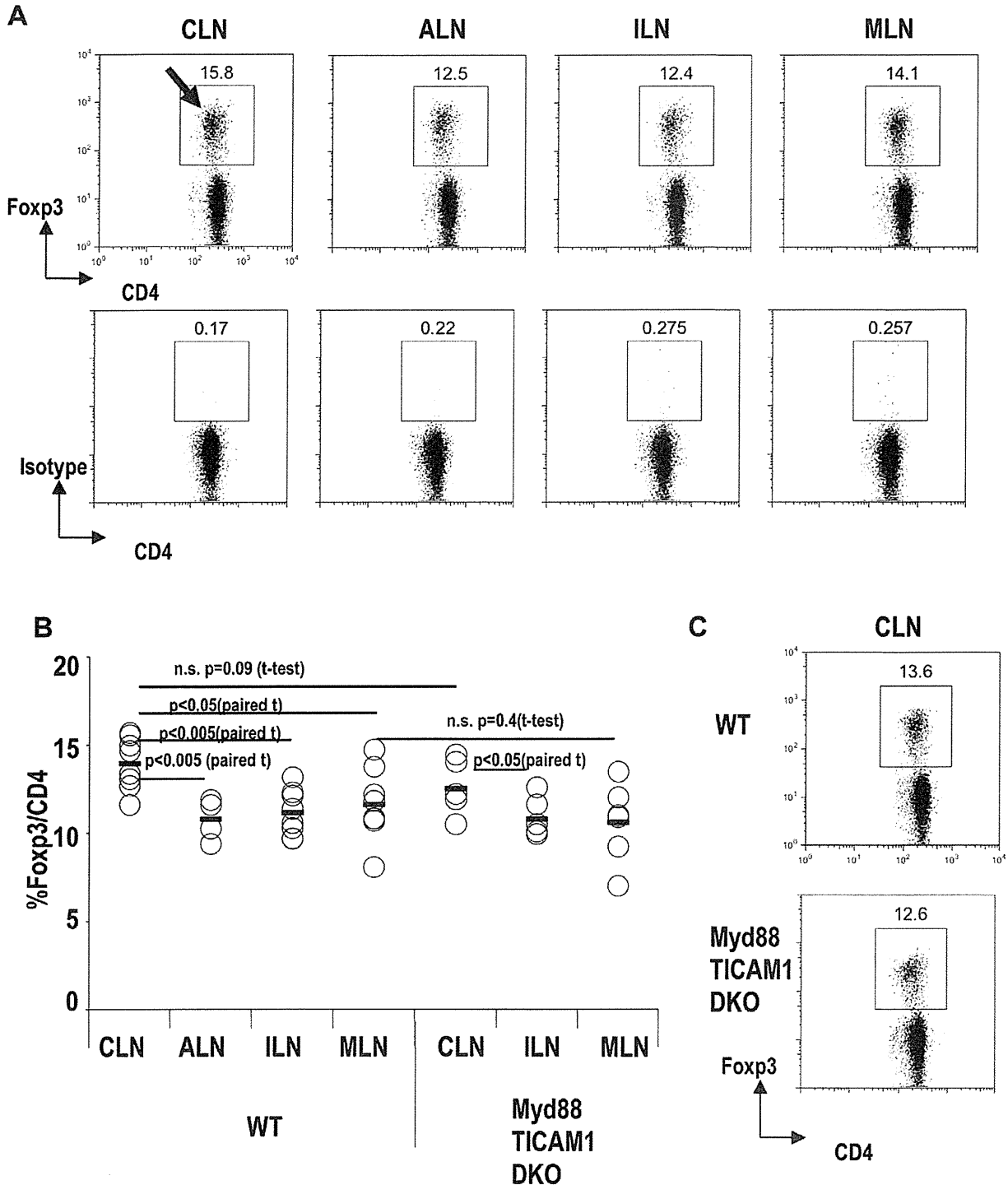

Figure 1. Frequency of Foxp3$^+$ T-regs in cervical lymph node is increased in a Myd88/TICAM-1 independent manner. (A) Cervical lymph nodes (CLN), axillary lymph nodes (ALN), inguinal lymph nodes (ILN), and mesenteric lymph nodes (MLN) from wild type B6 mice were analyzed for the expression of Foxp3. The isotype control is shown at the bottom. Plots were gated on CD4$^+$ T cells. Representative of seven separate experiments. (B) As in (A), but CLN, ALN, ILN and MLN from wild-type B6 mice (WT) or Myd88/TICAM1 double knockout mice (Myd88/TICAM1 DKO) were analyzed for the expression of Foxp3. Summary from seven separate experiments. P value provided is by paired t-test or t-test. "n.s."="not significant". (C) As in (B), but a representative of CLN is shown.
doi:10.1371/journal.pone.0051665.g001

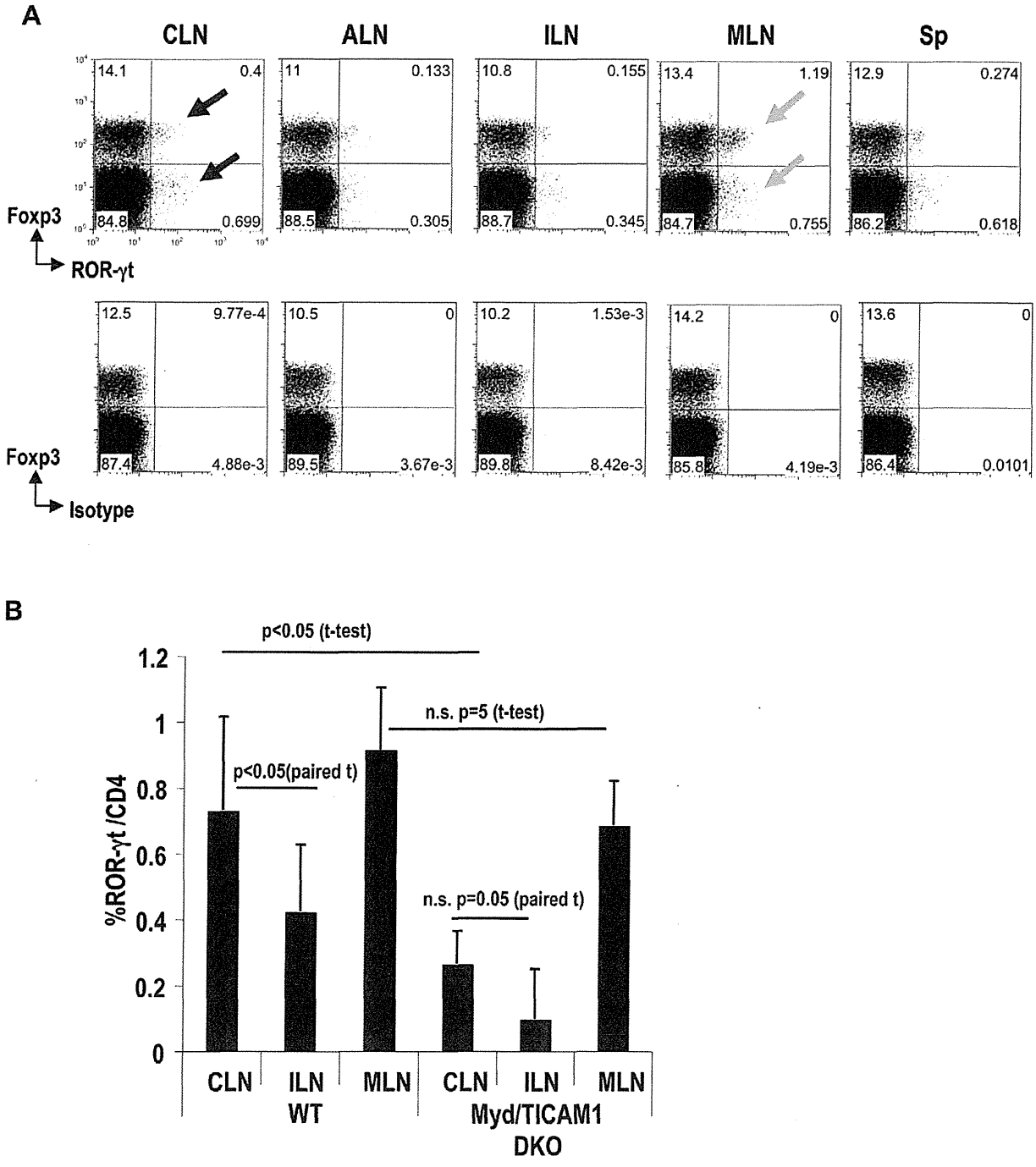

Figure 2. Frequency of ROR-γt$^+$CD4$^+$ T cell in cervical lymph node is increased in a Myd88/TICAM-1 dependent manner. (A) CLN, ALN, ILN, MLN, and spleen (Sp) from WT B6 mice were analyzed for the expression of Foxp3 and ROR-γt. The plots were gated on CD4$^+$ T cells. Isotype staining for ROR-γt is shown at the bottom. Representative of three separate experiments. (B) As in (A), but cells from WT mice or Myd88/TICAM-1 DKO mice were analyzed for the expression of ROR-γt and CD4. The graphic shows a summary from two separate experiments. P value provided is by paired-t test or t-test. "n.s." = "not significant".
doi:10.1371/journal.pone.0051665.g002

These results suggest that CD103$^+$ DCs and retinoic acid may not contribute to inducing Foxp3$^+$T-regs in CLNs. It is possible that the classical CD8$^-$ DC subset in CLNs may participate in the induction of Foxp3$^+$T-regs. Further studies are required.

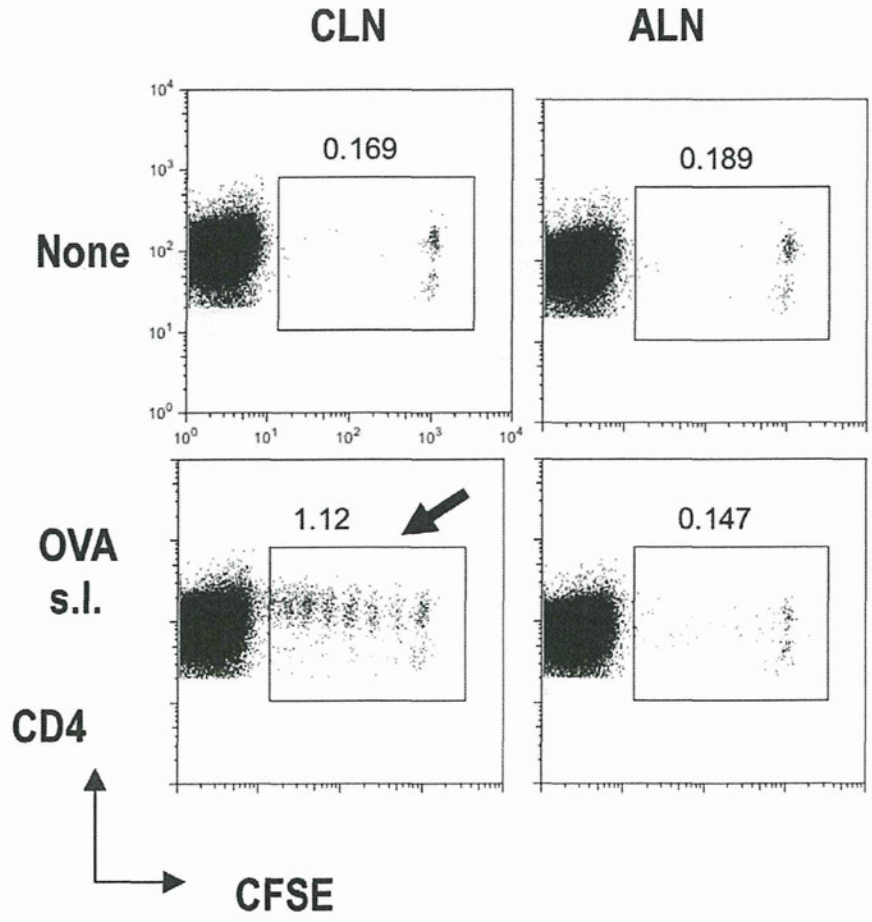

Figure 3. Cervical lymph nodes are draining lymph nodes from the oral cavity. CFSE-labeled OTII CD4+T cells were adoptively transferred into B6 mice on day −1. On day 0, 500 μg of OVA was administered sublingually (s.l.). CLN or ALN was analyzed for CFSE dilution at day 3. One of two similar experiments is shown for the FACS plots. Plots were gated on CD4+T cells.
doi:10.1371/journal.pone.0051665.g003

Discussion

The oral cavity is exposed to many antigens and commensal organisms every day [23,24,25,26]. The oral cavity is frequently associated with systemic immunological disorders, such as graft versus host diseases, Stevens-Johnson syndrome and Behçet diseases. However, it is unknown how tolerance in the oral cavity is maintained. Here, we showed that the balance between Th17 and Foxp3+T-regs may play a role in maintaining tolerance in the oral cavity. We found that the frequencies of Foxp3+T-regs and ROR-γt +CD4+T cells were increased in oral-cavity-draining CLNs, compared with skin-draining LNs and mesenteric LNs. DCs from oral-cavity-draining CLNs have the capacity to induce Foxp3+ T-regs *in vitro* on antigen stimulation, as much as DCs from mesenteric LNs do. These data suggest that the induced Foxp3+T-regs in oral-cavity-draining CLNs may be important in maintaining mucosal tolerance in response to microbes and food antigens in the oral cavity.

Although some TLR signaling is involved in inducing Foxp3+ T-regs [20,27,28,41,42], the high frequency of Foxp3+ T-regs in CLNs was not dependent on Myd88/TICAM1 (Fig. 1). Thus, TLR signaling is apparently not involved in the induction of Foxp3+T-regs in the oral cavity. However, we cannot exclude the possibility that some specific microbes may be involved in the inducing Foxp3+T-regs in the oral cavity in a Myd88/TICAM1 independent manner. For example, Atarashi et al recently showed that *Clostridum* induces Foxp3+T-regs in the colon in a Myd88-independent manner [19]. It might be interesting to investigate if there are specific microbes that contribute to the induction of Foxp3+T-regs in the oral cavity, especially as the bacterial community varies between the oral cavity and gut [26].

Our results showed that the high frequency of ROR-γt+CD4+T cells was dependent on Myd88/TICAM1 in the oral-cavity-draining CLNs (Fig.2). This is consistent with recent findings in skin [43]. Th17 cells in skin are reduced in Myd88/TICAM1 knockout mice and skin-resident commensal bacteria induce Th17 cells in a Myd88- and IL-1 receptor-dependent manner [43]. It is also known that some microbes induce Th17 using TLR signals; for example, Th17 cells induced by *Chlamydia* infection are reduced in Myd88 KO mice [44]. Thus, it is possible that TLR signals through some oral microbes are responsible for the increase of ROR-γt +CD4+T cells in oral-cavity-draining CLNs. Interestingly, the intestine may use a different mechanism from the oral cavity and skin to maintain Th17 cells, because Th17 cells are not reduced in the intestine in Myd88/TICAM1(TRIF)-knock out mice [45,46].

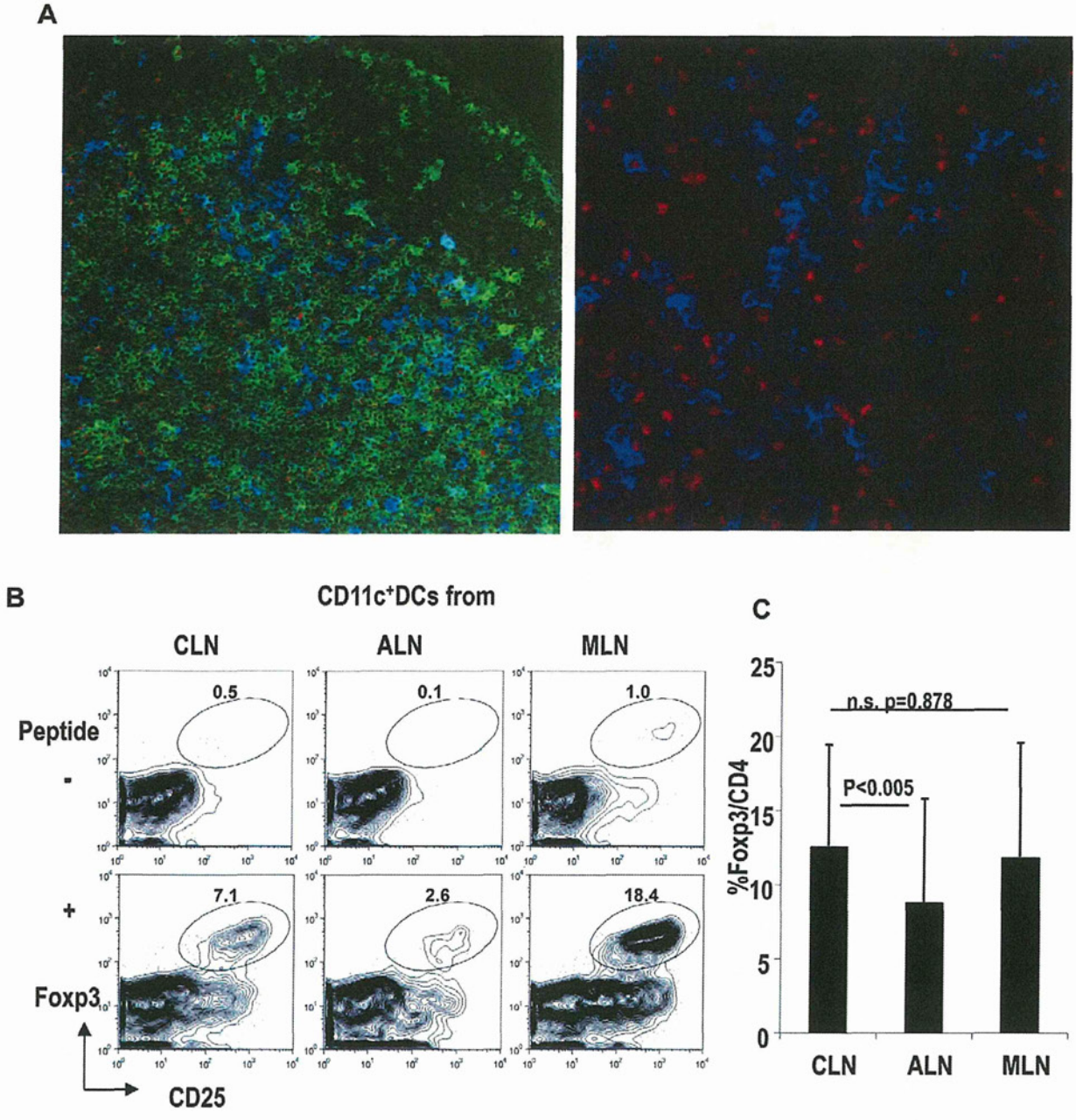

Figure 4. Dendritic cells from oral-cavity-draining cervical lymph nodes induce Foxp3$^+$ T-regs. (A) CLNs were stained with Foxp3 (red), CD4 (green) and CD11c (blue). Representative of three similar separate experiments. (B) OT II CD4$^+$ T cells (5×10^4) were cultured with dendritic cells (DCs) from CLN, ALN, or MLN (5×10^4) with or without OVA peptide. After 5 days, cells were stained with Foxp3, CD25 and CD4. The plots were gated on CD4$^+$ T cells. Representative of four separate experiments. (C) As in (A), but the graphic shows a summary of four separate experiments. P value provided is by paired t-test. "n.s." = "not significant".
doi:10.1371/journal.pone.0051665.g004

Furthermore, we found that DCs from oral-cavity-draining CLNs induce Foxp3$^+$T-regs in the presence of antigen, as do DCs from MLNs (Fig.4B). It has been reported that cutaneous CD103$^+$DCs induce Foxp3$^+$T-regs using RALDH2, as intestinal CD103$^+$DCs do [47]. Here, we would like to propose that DCs in the oral cavity use a different mechanism(s) to induce Foxp3$^+$Tregs from DCs in the intestine. First, CLNs have few CD103$^+$ DCs compared with MLNs (Fig. 5B). Second, DCs from CLNs do not express RALDH2 at the mRNA level (Fig. 5A). We have not yet found any specific DC subset in the oral-cavity-draining CLNs. However, CD8$^-$ classical DCs are increased in CLNs versus ALNs. Our previous report showed that CD8$^+$DEC205$^+$DCs induce Foxp3$^+$T-regs from Foxp3$^-$ cells and that CD8$^-$33D1$^+$DCs expand natural occurring Foxp3$^+$T-regs

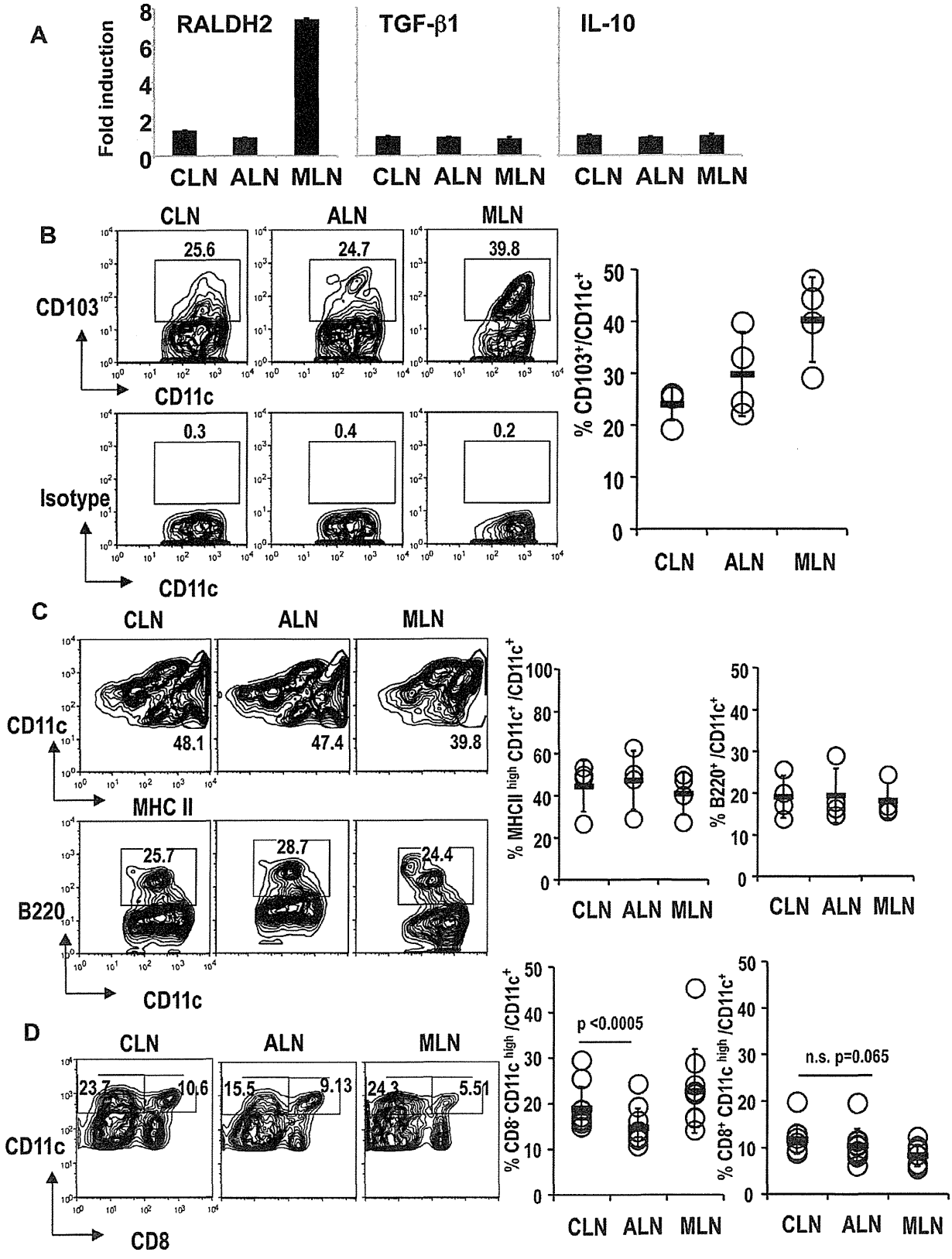
A
RALDH2
TGF-β1
IL-10
Fold induction
CLN ALN MLN
B
CLN
ALN
MLN
25.6
24.7
39.8
CD103
CD11c
0.3
0.4
0.2
Isotype
% CD103+/CD11c+
C
48.1
47.4
39.8
CD11c
MHC II
25.7
28.7
24.4
B220
% MHCII high CD11c+ /CD11c+
% B220+ /CD11c+
D
23.7
10.6
15.5
9.13
24.3
5.51
CD8
p <0.0005
n.s. p=0.065
% CD8- CD11c high /CD11c+
% CD8+ CD11c high /CD11c+

Figure 5. Phenotype of dendritic cells from cervical lymph nodes. (A) DCs from CLN, ALN, and MLN were freshly prepared from B6 mice. mRNA was prepared and real-time PCR was performed. Expression of each sample was normalized to GAPDH mRNA expression and fold increase of each sample was calculated relative to the expression at 0 h. One of two separate experiments is shown. (B) DCs from CLN, ALN, and MLN were analyzed for the expression of CD103. The plots were gated on $CD11c^+$ cells. The isotype control for CD103 is shown at the bottom. The graphic shows a summary of four separate experiments. Average +/− SD is shown. (C) As in (B), DCs from CLN, ALN, and MLN were analyzed for the expression of MHC class II or B220. The plots were gated on $CD11c^+$ cells. The graphic shows a summary of four separate experiments. Average +/− SD is shown. (D) As in (B), DCs from CLN, ALN, and MLN were analyzed for the expression of CD8. The plots were gated on $CD11c^+$ cells. The graphic shows a summary of 10 separate experiments. P value provided is by paired t-test. "n.s."="not significant".
doi:10.1371/journal.pone.0051665.g005

[6,11]. Thus, it seems possible that $CD8^-$DCs in CLNs may participate in expanding natural occurring $Foxp3^+$T-regs.

Recently, it has been reported that recently activated $Foxp3^+$T-regs from CLNs accumulated in CLNs after adoptive transfer [48]. It was suggested that TCR-mediated signals upon antigen stimulation may play a key role in the site-specific accumulation of $Foxp3^+$T-regs in CLNs. Taken together, oral-cavity-draining CLNs may be a special location where $Foxp3^+$T-regs are induced and also accumulate.

Here we showed that $Foxp3^+$T-regs are induced in oral-cavity-draining CLNs in a Myd88/TICAM1 independent manner and that DCs from oral-cavity-draining CLNs have the capacity to induce $Foxp3^+$Tregs on antigen stimulation. The mechanisms by which DCs to induce $Foxp3^+$T-regs may differ from those in the intestine. We propose that $Foxp3^+$T-regs play an important role in maintaining tolerance in the oral cavity to suppress Th17, as in the intestine. DCs from CLNs play a key role in maintaining tolerance upon oral antigen stimulation in the oral cavity. Further studies are required to identify the mechanism(s) by which DCs to induce $Foxp3^+$T-regs in the oral cavity.

Materials and Methods

Mice

C57BL6J (B6) mice were from Japan Clea (Tokyo). Myd88 KO mice were from Dr. Shizuo Akira (Osaka University). TICAM-1 KO mice were established in our laboratory [29,30]. OT-II OVA CD4 T cell receptor transgenic mice were kindly provided by Dr. Kazuya Iwabuchi (Kitasato University). The mice were maintained in the Hokkaido University Animal Facility in a specific pathogen-free condition. All experiments used mice between 6-12-week-old mice at the time of first procedure. All mice were used according to the guidelines of the institutional animal care and use committee of the Hokkaido University, who approved this study (ID number: 08-0243, "Analysis of immune modulation by toll-like receptors.").

Antibodies and Reagents

PE-conjugated CD103, CD25 (PC61), Alexa-488 conjugated anti-CD25 (7D4), FITC, biotin or APC conjugated CD4 (RM4-5), CD11c, B220, NK1.1, purified anti-CD16/CD32 (2.4G2) antibodies were from Biolegend (San Diego, CA). Anti-CD11c, and streptavidin microbeads were from Miltenyi Biotec (Gladbach, Germany). CFSE was from Molecular Probes (Eugene, OR). PE conjugated anti-mouse ROR-γt antibody and the anti-mouse Foxp3 (FJK-16s) staining kit were from eBioscience (San Diego, CA). LPS free OVA protein was from Seikagaku Co.(Tokyo, Japan).

Cell Isolation

$CD4^+$ T cells were first negatively separated by MACS beads from lymph nodes and spleen cell suspensions (>90%; Miltenyi Biotech). $CD4^+$ T cells were sometimes further purified by FACS Aria II (BD Bioscience, Franklin Lakes, NJ). $CD11c^+$ DCs from spleen, CLNs, ALNs, or MLNs were selected with anti-CD11c beads (Miltenyi Biotech) [7,10].

Co-culture with T cells and DCs

$CD4^+$T cells from OT II transgenic mice were cultured with DCs at 0 or 0.01-μM OVA peptide for 5 days. After 5 days, each culture was stained with Foxp3, following the manufacturer's protocol. Cells were acquired by FACS calibur flow cytometer (BD). Analyses were performed using the Flowjo software (TreeStar, USA).

Adoptive Transfer of OT-II $CD4^+$T cells

$CD4^+$T cells from OT II transgenic mice were labeled with 5 μM CFSE, and 1×10^6 T cells were injected intravenously into B6 recipients. One day later, OVA protein was administered sublingually. After 3 days, mice were sacrificed, and CLNs and ALNs were stained with CD4 and CFSE dilution was investigated. Cells were assessed by FACS calibur (BD). Analyses were performed using the Flowjo software (TreeStar, USA).

Quantitative PCR

Total RNA was isolated with TRIzol (Invitrogen), and reversed-transcribed with the High Capacity cDNA Transcription Kit (ABI) according to manufacturer's instructions. qPCR was performed with the Step One Real-Time PCR system (ABI). All primers for real-time PCR have been reported previously [27,28].

Measuring Cytokine Production

The purified DCs (1×10^5) were cultured in serum free RPMI medium for 20 h. The concentrations of TGF-ß in the supernatants were measured by TGF-ßELISA kit (R&D). Following the manufacturer's instructions, we measured the TGF-ß with or without activation of the latent form of TGF-ß. Culture supernatants with OT II $CD4^+$T cells and DCs were measured for IL-10 by ELISA (eBiosciences) or Cytometric Bead Array (BD Bioscience). Analysis with the Cytometric Bead Array was performed according to the manufacturer's instructions.

Confocal Microscopy

CLNs were sectioned, fixed with acetone, and stained with anti-CD4-FITC and CD11c-APC antibodies. After permeabilization with the buffer from the Foxp3 staining kit (eBioscience), they were stained with an anti-Foxp3-PE antibody. They were washed and observed by confocal microscopy (LSM510 META, Zeiss, Jena, Germany).

Supporting Information

Figure S1 $CD25^+$ and $CD25^-$ $Foxp3^+$ T-regs in lymph nodes and spleen. (A) CLN, ALN, ILN, MLN and Sp from B6 mice were analyzed for the expression of Foxp3 and CD25. The isotype control for Foxp3 is shown at the bottom. Plots were gated on $CD4^+$ T cells. Representative of 2 separate experiments is

shown. (B) As in (A), but the frequency of CD25$^+$ or CD25$^-$ Foxp3$^+$ T-regs/CD4+T cells were shown.
(TIF)

Figure S2 The frequency of CD11c$^+$ DC is similar between CLN and ALN. (A) CLN or ALN from one B6 mouse were digested by collagenase and stained with anti-CD11c and CD8 Abs. Representative of 5 separate experiments is shown. (B) The frequency of CD11c$^+$ cells/total LN cells in one mouse is shown. A summary of 5 separate experiments. P value provided is by paired t-test. "n.s." = "not significant".
(TIF)

Acknowledgments

We thank Dr. Kazuya Iwabuchi and Dr. Shizuo Akira for the mice. We appreciate Dr. Ralph M. Steinman (Rockefeller University) for his encouragement and visiting our lab. We thank for Ms. Akiko Nishioka and Ms.Saori Kasuya for their technical assistance.

Author Contributions

Conceived and designed the experiments: SY. Performed the experiments: A. Maruyama SY KO. Analyzed the data: SY A. Maruyama MM A. Morita TS. Wrote the paper: SY.

References

1. Sakaguchi S, Yamaguchi T, Nomura T, Ono M (2008) Regulatory T cells and immune tolerance. Cell 133: 775–787.
2. Sakaguchi S, Miyara M, Costantino CM, Hafler DA (2010) FOXP3+ regulatory T cells in the human immune system. Nature reviews Immunology 10: 490–500.
3. Rudensky AY (2011) Regulatory T cells and Foxp3. Immunological reviews 241: 260–268.
4. Bour-Jordan H, Bluestone JA (2009) Regulating the regulators: costimulatory signals control the homeostasis and function of regulatory T cells. Immunological reviews 229: 41–66.
5. Yamazaki S, Inaba K, Tarbell KV, Steinman RM (2006) Dendritic cells expand antigen-specific Foxp3+ CD25+ CD4+ regulatory T cells including suppressors of alloreactivity. Immunological reviews 212: 314–329.
6. Yamazaki S, Steinman RM (2009) Dendritic cells as controllers of antigen-specific Foxp3+ regulatory T cells. Journal of dermatological science 54: 69–75.
7. Yamazaki S, Iyoda T, Tarbell K, Olson K, Velinzon K, et al. (2003) Direct expansion of functional CD25+ CD4+ regulatory T cells by antigen-processing dendritic cells. The Journal of experimental medicine 198: 235–247.
8. Fehervari Z, Sakaguchi S (2004) Control of Foxp3+ CD25+CD4+ regulatory cell activation and function by dendritic cells. International immunology 16: 1769–1780.
9. Yamazaki S, Patel M, Harper A, Bonito A, Fukuyama H, et al. (2006) Effective expansion of alloantigen-specific Foxp3+ CD25+ CD4+ regulatory T cells by dendritic cells during the mixed leukocyte reaction. Proceedings of the National Academy of Sciences of the United States of America 103: 2758–2763.
10. Yamazaki S, Bonito AJ, Spisek R, Dhodapkar M, Inaba K, et al. (2007) Dendritic cells are specialized accessory cells along with TGF-ß for the differentiation of Foxp3+ CD4+ regulatory T cells from peripheral Foxp3 precursors. Blood 110: 4293–4302.
11. Yamazaki S, Dudziak D, Heidkamp GF, Fiorese C, Bonito AJ, et al. (2008) CD8+ CD205+ splenic dendritic cells are specialized to induce Foxp3+ regulatory T cells. Journal of immunology 181: 6923–6933.
12. Darrasse-Jeze G, Deroubaix S, Mouquet H, Victora GD, Eisenreich T, et al. (2009) Feedback control of regulatory T cell homeostasis by dendritic cells in vivo. The Journal of experimental medicine 206: 1853–1862.
13. Izcue A, Coombes JL, Powrie F (2009) Regulatory lymphocytes and intestinal inflammation. Annual review of immunology 27: 313–338.
14. Barnes MJ, Powrie F (2009) Regulatory T cells reinforce intestinal homeostasis. Immunity 31: 401–411.
15. Hand T, Belkaid Y (2010) Microbial control of regulatory and effector T cell responses in the gut. Current opinion in immunology 22: 63–72.
16. Coombes JL, Siddiqui KR, Arancibia-Carcamo CV, Hall J, Sun CM, et al. (2007) A functionally specialized population of mucosal CD103+ DCs induces Foxp3+ regulatory T cells via a TGF-beta and retinoic acid-dependent mechanism. The Journal of experimental medicine 204: 1757–1764.
17. Sun CM, Hall JA, Blank RB, Bouladoux N, Oukka M, et al. (2007) Small intestine lamina propria dendritic cells promote de novo generation of Foxp3 T reg cells via retinoic acid. The Journal of experimental medicine 204: 1775–1785.
18. Manicassamy S, Reizis B, Ravindran R, Nakaya H, Salazar-Gonzalez RM, et al. (2010) Activation of beta-catenin in dendritic cells regulates immunity versus tolerance in the intestine. Science 329: 849–853.
19. Atarashi K, Tanoue T, Shima T, Imaoka A, Kuwahara T, et al. (2011) Induction of colonic regulatory T cells by indigenous Clostridium species. Science 331: 337–341.
20. Round JL, Lee SM, Li J, Tran G, Jabri B, et al. (2011) The Toll-like receptor 2 pathway establishes colonization by a commensal of the human microbiota. Science 332: 974–977.
21. Huber S, Gagliani N, Esplugues E, O'Connor W Jr, Huber FJ, et al. (2011) Th17 cells express interleukin-10 receptor and are controlled by Foxp3- and Foxp3+ regulatory CD4+ T cells in an interleukin-10-dependent manner. Immunity 34: 554–565.
22. Chaudhry A, Samstein RM, Treuting P, Liang Y, Pils MC, et al. (2011) Interleukin-10 signaling in regulatory T cells is required for suppression of Th17 cell-mediated inflammation. Immunity 34: 566–578.
23. Avila M, Ojcius DM, Yilmaz O (2009) The oral microbiota: living with a permanent guest. DNA and cell biology 28: 405–411.
24. Sansonetti PJ (2011) To be or not to be a pathogen: that is the mucosally relevant question. Mucosal immunology 4: 8–14.
25. Grice EA, Kong HH, Conlan S, Deming CB, Davis J, et al. (2009) Topographical and temporal diversity of the human skin microbiome. Science 324: 1190–1192.
26. Costello EK, Lauber CL, Hamady M, Fierer N, Gordon JI, et al. (2009) Bacterial community variation in human body habitats across space and time. Science 326: 1694–1697.
27. Manicassamy S, Ravindran R, Deng J, Oluoch H, Denning TL, et al. (2009) Toll-like receptor 2-dependent induction of vitamin A-metabolizing enzymes in dendritic cells promotes T regulatory responses and inhibits autoimmunity. Nature medicine 15: 401–409.
28. Yamazaki S, Okada K, Maruyama A, Matsumoto M, Yagita H, et al. (2011) TLR2-dependent induction of IL-10 and Foxp3+CD25+CD4+ regulatory T cells prevents effective anti-tumor immunity induced by Pam2 lipopeptides in vivo. PloS One 6: e18833.
29. Oshiumi H, Matsumoto M, Funami K, Akazawa T, Seya T (2003) TICAM-1, an adaptor molecule that participates in Toll-like receptor 3-mediated interferon-beta induction. Nature immunology 4: 161–167.
30. Akazawa T, Ebihara T, Okuno M, Okuda Y, Shingai M, et al. (2007) Antitumor NK activation induced by the Toll-like receptor 3-TICAM-1 (TRIF) pathway in myeloid dendritic cells. Proceedings of the National Academy of Sciences of the United States of America 104: 252–257.
31. Mucida D, Park Y, Kim G, Turovskaya O, Scott I, et al. (2007) Reciprocal TH17 and regulatory T cell differentiation mediated by retinoic acid. Science 317: 256–260.
32. Ivanov, II, McKenzie BS, Zhou L, Tadokoro CE, Lepelley A, et al. (2006) The orphan nuclear receptor RORgammat directs the differentiation program of proinflammatory IL-17+ T helper cells. Cell 126: 1121–1133.
33. Onodera T, Jang MH, Guo Z, Yamasaki M, Hirata T, et al. (2009) Constitutive expression of IDO by dendritic cells of mesenteric lymph nodes: functional involvement of the CTLA-4/B7 and CCL22/CCR4 interactions. Journal of immunology 183: 5608–5614.
34. Ochando JC, Homma C, Yang Y, Hidalgo A, Garin A, et al. (2006) Alloantigen-presenting plasmacytoid dendritic cells mediate tolerance to vascularized grafts. Nature immunology 7: 652–662.
35. Hanabuchi S, Ito T, Park WR, Watanabe N, Shaw JL, et al. (2010) Thymic stromal lymphopoietin-activated plasmacytoid dendritic cells induce the generation of FOXP3+ regulatory T cells in human thymus. Journal of immunology 184: 2999–3007.
36. Chen W, Liang X, Peterson AJ, Munn DH, Blazar BR (2008) The indoleamine 2,3-dioxygenase pathway is essential for human plasmacytoid dendritic cell-induced adaptive T regulatory cell generation. Journal of immunology 181: 5396–5404.
37. Seneschal J, Clark RA, Gehad A, Baecher-Allan CM, Kupper TS (2012) Human epidermal Langerhans cells maintain immune homeostasis in skin by activating skin resident regulatory T cells. Immunity 36: 873–884.
38. Azukizawa H, Dohler A, Kanazawa N, Nayak A, Lipp M, et al. (2011) Steady state migratory RelB+ langerin+ dermal dendritic cells mediate peripheral induction of antigen-specific CD4+ CD25+ Foxp3+ regulatory T cells. European journal of immunology 41: 1420–1434.
39. Kautz-Neu K, Noordegraaf M, Dinges S, Bennett CL, John D, et al. (2011) Langerhans cells are negative regulators of the anti-Leishmania response. The Journal of experimental medicine 208: 885–891.
40. Gomez de Aguero M, Vocanson M, Hacini-Rachinel F, Taillardet M, Sparwasser T, et al. (2012) Langerhans cells protect from allergic contact dermatitis in mice by tolerizing CD8+ T cells and activating Foxp3+ regulatory T cells. The Journal of clinical investigation 122: 1700–1711.
41. Sutmuller RP, den Brok MH, Kramer M, Bennink EJ, Toonen LW, et al. (2006) Toll-like receptor 2 controls expansion and function of regulatory T cells. The Journal of clinical investigation 116: 485–494.
42. Round JL, Mazmanian SK (2010) Inducible Foxp3+ regulatory T-cell development by a commensal bacterium of the intestinal microbiota. Proceedings of the National Academy of Sciences of the United States of America 107: 12204–12209.

43. Naik S, Bouladoux N, Wilhelm C, Molloy MJ, Salcedo R, et al. (2012) Compartmentalized Control of Skin Immunity by Resident Commensals. Science.
44. Zhang X, Gao L, Lei L, Zhong Y, Dube P, et al. (2009) A MyD88-dependent early IL-17 production protects mice against airway infection with the obligate intracellular pathogen Chlamydia muridarum. Journal of immunology 183: 1291–1300.
45. Atarashi K, Nishimura J, Shima T, Umesaki Y, Yamamoto M, et al. (2008) ATP drives lamina propria T(H)17 cell differentiation. Nature 455: 808–812.
46. Ivanov, II, Atarashi K, Manel N, Brodie EL, Shima T, et al. (2009) Induction of intestinal Th17 cells by segmented filamentous bacteria. Cell 139: 485–498.
47. Guilliams M, Crozat K, Henri S, Tamoutounour S, Grenot P, et al. (2010) Skin-draining lymph nodes contain dermis-derived CD103- dendritic cells that constitutively produce retinoic acid and induce Foxp3+ regulatory T cells. Blood 115: 1958–1968.
48. Lieberman SM, Kim JS, Corbo-Rodgers E, Kambayashi T, Maltzman JS, et al. (2012) Site-specific accumulation of recently activated CD4+ Foxp3+ regulatory T cells following adoptive transfer. European journal of immunology 42: 1429–1435.

Toll-like receptor 3 signaling converts tumor-supporting myeloid cells to tumoricidal effectors

Hiroaki Shime[a], Misako Matsumoto[a], Hiroyuki Oshiumi[a], Shinya Tanaka[b], Akio Nakane[c], Yoichiro Iwakura[d], Hideaki Tahara[e], Norimitsu Inoue[f], and Tsukasa Seya[a,1]

[a]Department of Microbiology and Immunology, and [b]Department of Cancer Pathology, Graduate School of Medicine, Hokkaido University, Kita-ku, Sapporo 060-8638, Japan; [c]Department of Microbiology and Immunology, Graduate School of Medicine, Hirosaki University, Zaifu-cho, Hirosaki 036-8562, Japan; [d]Laboratory of Molecular Pathogenesis, Center for Experimental Medicine and Systems Biology, and [e]Department of Surgery and Bioengineering, Advanced Clinical Research Center, Institute of Medical Science, University of Tokyo, Shirokanedai, Minato-ku, Tokyo 108-8639, Japan; and [f]Department of Molecular Genetics, Osaka Medical Center for Cancer, Nakamichi, Higashinari-ku, Osaka 537-8511, Japan

Edited by Ruslan Medzhitov, Yale University School of Medicine, New Haven, CT, and approved December 20, 2011 (received for review August 11, 2011)

Smoldering inflammation often increases the risk of progression for malignant tumors and simultaneously matures myeloid dendritic cells (mDCs) for cell-mediated immunity. PolyI:C, a dsRNA analog, is reported to induce inflammation and potent antitumor immune responses via the Toll-like receptor 3/Toll–IL-1 receptor domain-containing adaptor molecule 1 (TICAM-1) and melanoma differentiation-associated protein 5/IFN-β promoter stimulator 1 (IPS-1) pathways in mDCs to drive activation of natural killer cells and cytotoxic T lymphocytes. Here, we found that i.p. or s.c. injection of polyI:C to Lewis lung carcinoma tumor-implant mice resulted in tumor regression by converting tumor-supporting macrophages (Mfs) to tumor suppressors. F4/80$^+$/Gr1$^-$ Mfs infiltrating the tumor respond to polyI:C to rapidly produce inflammatory cytokines and thereafter accelerate M1 polarization. TNF-α was increased within 1 h in both tumor and serum upon polyI:C injection into tumor-bearing mice, followed by tumor hemorrhagic necrosis and growth suppression. These tumor responses were abolished in TNF-α$^{-/-}$ mice. Furthermore, F4/80$^+$ Mfs in tumors extracted from polyI:C-injected mice sustained Lewis lung carcinoma cytotoxic activity, and this activity was partly abrogated by anti–TNF-α Ab. Genes for supporting M1 polarization were subsequently up-regulated in the tumor-infiltrating Mfs. These responses were completely abrogated in TICAM-1$^{-/-}$ mice, and unaffected in myeloid differentiation factor 88$^{-/-}$ and IPS-1$^{-/-}$ mice. Thus, the TICAM-1 pathway is not only important to mature mDCs for cross-priming and natural killer cell activation in the induction of tumor immunity, but also critically engaged in tumor suppression by converting tumor-supporting Mfs to those with tumoricidal properties.

Toll-like receptor | tumor-associated macrophages | TRIF

Inflammation followed by bacterial and viral infections triggers a high risk of cancer and promotes tumor development and progression (1, 2). Long-term use of anti-inflammatory drugs has been shown to reduce—if not eliminate—the risk of cancer, as demonstrated by a clinical study of aspirin and colorectal cancer occurrence (3). Inflammatory cytokines facilitate tumor progression and metastasis in most cases. Innate immune response and the following cellular events are closely concerned with the formation of the tumor microenvironment (4, 5).

By contrast, inflammation induced by microbial preparations was applied to patients with cancer for therapeutic potential as Coley vaccine with some success. A viral replication product, dsRNA and its analog polyI:C (6, 7), induced acute inflammation, and has been expected to be a promising therapeutic agent against cancer. Although polyI:C exerts life-threatening cytokinemia (8), trials for its clinical use as an adjuvant continued because of its high therapeutic potential (9, 10). Pathogen-associated molecular patterns (PAMPs) and host cell factors induced secondary to PAMP–host cell interaction act as a double-edged sword in cancer prognosis and require understanding their multifarious functional properties in the tumor environment.

Recent advances in the study of innate immunity show how polyI:C suppresses tumor progression (11). PolyI:C is a synthetic compound that serves as an agonist for pattern-recognition receptors (PRRs), Toll-like receptor 3 (TLR3), and melanoma differentiation-associated protein 5 (MDA5) (12–14). Although TLR3 and MDA5 signals are characterized as myeloid differentiation factor 88 (MyD88) independent (15, 16), they have immune effector-inducing properties (12–14, 17). TLR3 couples with the Toll–IL-1 receptor domain-containing adaptor molecule 1 (TICAM-1, also known as TRIF), and MDA5 couples with the IFN-β promoter stimulator 1 (IPS-1, also known as Cardif, MAVS, or VISA) (11, 15). Possible functions for the TICAM-1 and IPS-1 signaling pathways have been investigated by using gene-disrupted mice (15); although they activate the same downstream transcription factors NF-κB and IFN regulatory factor 3 (IRF-3) (15, 18), they appear to distinctly modulate myeloid dendritic cells (mDCs) and macrophages (Mfs) to drive effector lymphocytes (19, 20).

Tumor microenvironments frequently involve myeloid-derived suppressor cells (MDSCs), tumor-associated macrophages (TAMs), and immature mDCs (1, 21). These myeloid cells express PRR through which they are functionally activated. Once the inflammation process is triggered, immature mDCs turn mature so that they are capable of antigen cross-presentation and able to activate immune effector cells, which would act to protect the host system and damage the undesirable tumor cells (22). However, TAMs and MDSCs play a major role in establishing a favorable environment for tumor cell development by suppressing antitumor immunity and recruiting host immune cells to support tumor cell survival, motility, and invasion (23–25). Although these myeloid cell scenarios have been studied with interest, how the PRR signal in these myeloid cells links regulation of tumor progression has yet to be elucidated.

Here we show that TICAM-1 but not IPS-1 signal in tumor-infiltrating Mfs is engaged in conversion of the TAM-like Mfs to tumoricidal effectors. We investigated the molecular mechanisms in Mfs underlying the phenotype switch from tumor supporting to tumor suppressing by treating cells with polyI:C and found that the TICAM-1–inducing TNF-α and M1 polarization are crucial for eliciting tumoricidal activity in TAMs.

Results

In Vivo Effect of PolyI:C on Implant Lewis Lung Carcinoma Tumor. I.p. injection of polyI:C rapidly induced hemorrhagic necrosis in 3LL tumors implanted in WT mice, which was established >12 h after polyI:C treatment (Fig. 1*A*). The polyI:C-dependent hemorrhagic necrosis did not occur in TNF-α$^{-/-}$ mice (Fig. 1*A*). Histological

Author contributions: H.S., M.M., and T.S. designed research; H.S., H.O., and S.T. performed research; H.O., A.N., Y.I., and H.T. contributed new reagents/analytic tools; M.M. and N.I. analyzed data; and H.S. and T.S. wrote the paper.

The authors declare no conflict of interest.

This article is a PNAS Direct Submission.

[1]To whom correspondence should be addressed. E-mail: seya-tu@pop.med.hokudai.ac.jp.

This article contains supporting information online at www.pnas.org/lookup/suppl/doi:10.1073/pnas.1113099109/-/DCSupplemental.

and immunohistochemical analysis revealed vascular damage in the necrotic lesion, where disruption of vascular endothelial cells was indicated by fragmented $CD31^+$ marker (Fig. S1). Although the polyI:C signal is delivered by TICAM-1 and IPS-1 adaptors (11, 13), the hemorrhagic necrosis was largely alleviated in TICAM-$1^{-/-}$ mice but not in IPS-$1^{-/-}$ mice (Fig. 1*A*). The results suggest that polyI:C is a reagent that induces Lewis lung carcinoma (3LL) hemorrhagic necrosis, and the TICAM-1 pathway and its products, including TNF-α, are preferentially involved in this response.

3LL implant tumors grew well in WT C57BL6 mice. PolyI:C, when i.p. injected, resulted in tumor growth retardation (Fig. 1*B*). The retardation of tumor growth by polyI:C was also impaired in TNF-$\alpha^{-/-}$ mice (Fig. 1*B*), suggesting that TNF-α is a critical effector for not only induction of hemorrhagic necrosis but also further 3LL tumor regression. To investigate the signaling pathway involved in the tumor growth retardation by polyI:C, we challenged WT, MyD88$^{-/-}$, TICAM-$1^{-/-}$, and IPS-$1^{-/-}$ mice with 3LL implantation and then treated the mice with i.p. injection of polyI:C. 3LL growth retardation was observed in both IPS-$1^{-/-}$ (Fig. 1*C*) and MyD88$^{-/-}$ mice, to a similar extent to WT mice. In contrast, polyI:C-dependent tumor growth retardation was abrogated in TICAM-$1^{-/-}$ mice (Fig. 1*D*). The size differences of the implanted tumors became significant within 2 d after polyI:C treatment, suggesting that the molecular effector for tumor regression is induced early and its upstream is TICAM-1. Similar results were obtained with MC38 implant tumor (Fig. S2*A*), which is TNF-α sensitive and MHC class I positive (Table S1) (26).

PolyI:C is a reagent that induces natural killer (NK) cell activation in MHC class I-negative tumors (12), and 3LL cells are class I negative and NK cell sensitive (Table S1) (27, 28). We tested whether NK cells activated by polyI:C damage the 3LL tumor in mice. Tumor growth was not affected by pretreatment of the mice with anti-NK1.1 Ab in this model (Fig. S3). Thus, NK cells, at least the $NK1.1^+$ cells, have a negligible ability to retard tumor growth in vivo.

PolyI:C Induces TNF-α Through the TICAM-1 Pathway in Mice. To test whether polyI:C treatment had elicited TNF-α production in vivo, we investigated the cytokine profiles of serum from polyI:C-stimulated WT and IPS-$1^{-/-}$ and TICAM-$1^{-/-}$ mice by ELISA. Prominent differences in TNF-α levels were observed in serum collected from polyI:C-injected WT and TICAM-$1^{-/-}$ mice. Serum TNF-α levels in WT and IPS-$1^{-/-}$ mice were significantly higher than that in TICAM-$1^{-/-}$ mice within 1 h after polyI:C injection (Fig. S4 *A* and *B*). IFN-β is a main output for polyI:C stimulation (11), and its production was decreased in TICAM-$1^{-/-}$ mice and totally abrogated in IPS-$1^{-/-}$ mice (Fig. S4*C*). Taken together, the data indicate that the TICAM-1 pathway was able to sustain a high TNF-α level in the early phase of polyI:C treatment, which is independent of IPS-1 and subsequent production of IFN-β.

TICAM-1^+ Cells in Tumor Produces TNF-α in Response to PolyI:C Stimulation. Using the 3LL implant WT, IPS-$1^{-/-}$, and TICAM-$1^{-/-}$ mouse models, we tested whether polyI:C-induced early TNF-α was responsible for the lately observed tumor regression. Time-course analyses of the polyI:C-induced TNF-α protein levels were performed by ELISA using serum samples and tumors extracted from the experimental mice. The tumor TNF-α levels in WT and IPS-$1^{-/-}$ mice increased at 2 h after polyI:C i.p. injection (Fig. 2*A*). The serum TNF-α levels in both were rapidly up-regulated within 1 h after polyI:C injection, although in WT the levels continued to increase but in IPS-$1^{-/-}$ mice gradually decreased (Fig. 2*B*). In TICAM-$1^{-/-}$ mice, however, no appreciable up-regulation of TNF-α protein was detected in either tumor or serum samples during the early time-course tested. To test whether the induced TNF-α protein was generated de novo in tumors, we examined the corresponding mRNA levels in excised tumors (Fig. 2*C* and Table S2). The TNF-α mRNA levels peaked between 1 and 2 h after polyI:C injection, whereas the TNF-α protein level was kept high at >2 h after polyI:C injection in tumor as well as serum. In the TICAM-$1^{-/-}$ mice, TNF-α production was largely abrogated in the tumor and serum samples, suggesting that TNF-α was mainly produced and secreted in response to polyI:C stimulation from the TLR3/TICAM-1^+ cells within the tumor.

F4/80$^+$/Gr-1$^-$ Mfs in 3LL Tumor Produce TNF-α Leading to Tumor Damage. We next investigated the cell types that had infiltrated the tumor by using various Mf markers in FACS analysis and tumor samples extracted at 1 h after polyI:C injection. We discovered that $CD45^+$ cells in the tumor produced TNF-α in response to polyI:C (Fig. 3*A*). The major population of those $CD45^+$ cells was determined to be of $CD11b^+$ myeloid-lineage cells that coexpressed $F4/80^+$, $Gr1^+$, or $CD11c^+$. A small population of $NK1.1^+$ cells was also detected. $CD4^+$ T cells, $CD8^+$ T cells, and B cells were rarely detected in these implant tumors (Fig. S5*A*). Moreover, $F4/80^+$/Gr-1^- cells were found to be the principal contributors to polyI:C-mediated TNF-α production (Fig. 3 *B* and *C*). $F4/80^+$ cells in 3LL tumor highly expressed macrophage mannose receptor (MMR; CD206), a M2 macrophage marker, in contrast to splenic $F4/80^+CD11b^+$ cells. Both TNF-α–producing and –nonproducing $F4/80^+$ cell populations in 3LL tumor showed indistinguishable levels of CD206 (Fig. S6), and dissimilar to MDSCs or splenic Mfs, as determined by the surface marker profiles (Table S3). Thus, the source of the TNF-α–producing cells in tumor is likely $F4/80^+$ Mfs with a TAM-like feature.

We harvested $F4/80^+$ cells from tumor samples extracted from WT and TICAM-$1^{-/-}$ mice at 30 min after polyI:C injection. These cells were used in in vitro experiments to verify the TNF-α–producing abilities and 3LL cytotoxicity properties (Fig. 4 *A* and *B*). WT $F4/80^+$ Mfs exhibited normal TNF-α–producing function and were able to kill 3LL cells upon exposure. This tumoricidal activity was ~50% neutralized by the addition of anti–TNF-α Ab (Fig. 4*C*), although incomplete inhibition by this mAb may reflect participation of other factors in TNF-α cytotoxicity. Furthermore, when active TNF-α protein (rTNF-α) was added exogenously to 3LL cell culture, the cytotoxic effects were still present and occurred in a dose-dependent manner (Fig. 4*D*). TNF-α–producing ability was also observed in $F4/80^+$ cells from implant tumor of MC38, B16D8, or EL4, and only the MC38 tumor was remediable by TICAM-1–derived TNF-α (Fig. S2 *B* and *C*). The MC38 tumor contained the $F4/80^+$/$CD11b^+$/$Gr1^-$ cells, as in the 3LL tumor (Fig. S5*B*).

IFN-β did not enhance rTNF-α–mediated 3LL killing efficacy (Fig. S7*A*), a finding that was consistent with previously published data (29). No effect of IRF3/7 on polyI:C-induced 3LL tumor regression in vivo was confirmed using IRF3/7 double-knockout mice. However, polyI:C-dependent tumor regression was abrogated in 3LL-bearing IFN-α/β receptor (IFNAR)$^{-/-}$ mice (Fig. S7*B*). Quantitative PCR analysis of cells from WT vs. IFNAR$^{-/-}$ tumor-bearing mice revealed that the TLR3 level was basally low and not up-regulated in response to polyI:C in tumor-infiltrating $F4/80^+$ Mfs of IFNAR$^{-/-}$ mice (Fig. S7*C*). Accordingly, the TNF-α level was not up-regulated in tumor and serum in polyI:C-stimulated IFNAR$^{-/-}$ mice (Fig. S7*D*). Thus, basal induction of type I IFN serves as a critical factor for TLR3 function in tumor $F4/80^+$ Mfs to produce TNF-α in vivo. These results suggest that the direct effector for 3LL cytolysis by polyI:C involves TNF-α, which is derived from TICAM-1 downstream independent of the IRF3/7 axis. Our results indicate that cytotoxic TNF-α is produced via a distinct route from initial type I IFN and downstream of TICAM-1 in $F4/80^+$ TAM-like Mfs. Type I IFN do not synergistically act with TNF-α on 3LL killing, but is required to complete the TLR3/TICAM-1 pathway.

These results were confirmed by in vitro assay, wherein the $F4/80^+$ Mfs harvested from 3LL tumors in WT, TICAM-$1^{-/-}$, IPS-$1^{-/-}$, and TLR3$^{-/-}$ mice were stimulated with polyI:C (Fig. S8*A*). Both TNF-α release and 3LL cytotoxic abilities of polyI:C-stimulated $F4/80^+$ Mfs were specifically abrogated by the absence of TICAM-1 and TLR3 (Fig. S8 *A* and *B*). IPS-1 or

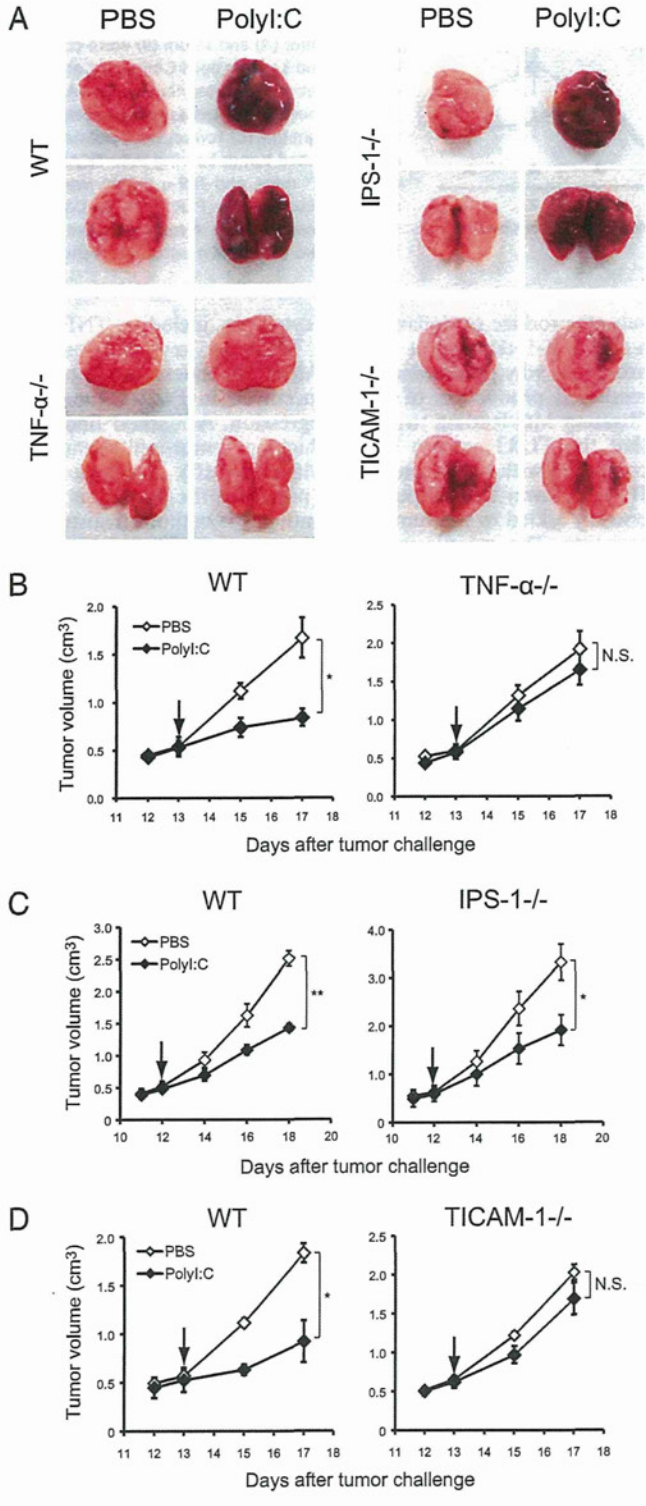

Fig. 1. Antitumor activity of polyI:C against 3LL tumor cells is mediated by the TICAM-1 pathway in vivo. (*A*) Representative photographs of 3LL tumors excised from WT, TNF-$\alpha^{-/-}$, TICAM-$1^{-/-}$, and IPS-$1^{-/-}$ mice. Whole tumor (*Upper*) and bisected tumor (*Lower*) are shown. (*B–D*) On day 0, 3LL tumor cells (3×10^6) were s.c. implanted into B6 WT (*B–D*), TNF-$\alpha^{-/-}$ (*B*), TICAM-$1^{-/-}$ (*C*), and IPS-$1^{-/-}$ (*D*) mice. PolyI:C i.p. injection was started on the day indicated by arrow, then repeated every 4 d. Data are shown as tumor average size ± SE; $n = 3$–4 mice per group. $^*P < 0.05$; $^{**}P < 0.001$. N.S., not significant. A representative experiment of two with similar outcomes is shown.

MyD88 in F4/80$^+$ Mfs had no or minimal effect on the TNF-α tumoricidal effect against 3LL tumors. PolyI:C did not directly exert a cytotoxic effect on 3LL tumor cells (Fig. S8*C*).

Role of the IPS-1 Pathway in F4/80$^+$ Cells. Both TICAM-1 and IPS-1 are known to converge their signals on transcription factors NF-κB and IRF-3, which drive expression of TNF-α and IFN-β, respectively. PolyI:C-induced TNF-α production was reduced in F4/80$^+$ cells extracted from tumors of TICAM-$1^{-/-}$ mice, but not in samples of IPS-$1^{-/-}$ mice. We examined the expression of IFN-β in these cells after polyI:C stimulation. Compared with F4/80$^+$ cells from WT mice, IFN-β expression and production was barely decreased in IPS-$1^{-/-}$ F4/80$^+$ cells, but largely impaired in TICAM-$1^{-/-}$ F4/80$^+$ cells (Fig. S9*A*) as other cytokines tested. M1 Mf-associated cytokines/chemokines were generally reduced in TICAM-$1^{-/-}$ F4/80$^+$ cells compared with WT and IPS-$1^{-/-}$ cells >4 h after polyI:C stimulation (Fig. S9*A*), whereas M2 Mf-associated genes were barely affected by TICAM-1 disruption or polyI:C stimulation (Fig. S9*B*).

Most types of Mfs are known to express TLR3 in mice (30). Messages and proteins for type I IFN induction were conserved in the F4/80$^+$ tumor-infiltrating Mfs (Fig. S10 *A–C*). However, the TLR3 mRNA level was low in macrophage colony-stimulating factor (M-CSF)–derived Mfs compared with TAMs (Fig. S10*D*). We further examined whether IFN-β production might also have relied on the TICAM-1 pathway in other types of Mfs upon stimulation with polyI:C. In contrast to the F4/80$^+$ cells isolated from tumor (Fig. S11 *A* and *B*), the IPS-1 pathway was indispensable for polyI:C-mediated IFN-β production in mouse peritoneal Mfs and M-CSF–induced bone marrow-derived Mfs (Fig. S11 *C* and *E*). However, IPS-1 only slightly participated in polyI:C-mediated TNF-α production in these Mf subsets (Fig. S11 *D* and *F*). It appears then that the IPS-1 pathway is able to signal the presence of polyI:C and subsequently induce type I IFN. TICAM-1 is the protein that induces effective TNF-α in all subsets of Mfs.

PolyI:C Influences Polarization of TAMs. Plasticity is a characteristic feature of Mfs (25). Various factors and signals can influence polarization of Mf cells to induce the M1/M2 transition, which is accompanied by a substantial change in the Mf cell's expression profile of cytokines and chemokines. Previous studies have demonstrated that Mfs that have infiltrated into tumor are of the M2-polarized phenotype, which is known to contribute to tumor progression. To test the effects of polyI:C on the polarization of tumor-infiltrated Mf cells, we analyzed the gene expression profiles of these cells following in vitro polyI:C stimulation, and representative profiles were confirmed by quantitative PCR (Fig. 5 *A* and *B*). The mRNA expressions were increased for M1 Mf markers IL-12p40, IL-6, CXCL11, and IL-1β at 4 h after in vitro polyI:C treatment, as were mRNA levels of IFN-β and TNF-α and ex vivo results. The M2 Mf markers arginase-1 (*Arg1*), chitinase 3-like 3 (*Chi3l3*), and MMR (*Mrc1*) were unchanged, compared with unstimulated levels; however, the M2 Mf marker IL-10, a regulatory cytokine, was induced. In addition, there was no difference observed in the mRNA expression levels of MMP9 (*Mmp9*) and VEGFA (*Vegfa*), both of which are involved in tissue remodeling and angiogenesis events of tumor progression (Fig. 5*C*). The polyI:C-induced M1 markers and IL-10 expression that were upregulated in WT and IPS-$1^{-/-}$ F4/80$^+$ cells were found to be abrogated in TICAM-$1^{-/-}$ F4/80$^+$ cells (Fig. 5 *A* and *B*), reinforcing the results obtained with F4/80$^+$ Mfs isolated from 3LL tumors in mice injected with polyI:C (Fig. S9 *A* and *B*). It appears that TICAM-1 is responsible for the M1 polarization of F4/80$^+$ Mf cells in tumors, but has no effect on M2 markers. We further examined the expression of IRF-5 and IRF-4, which are considered the master regulators for M1 and M2 polarization, respectively (31, 32). As expected, polyI:C induced IRF-5 mRNA expression, but had no effect on IRF-4 mRNA expression in vitro (Fig. 5 *A* and *B*). Jmjd3, a histone H3K27 demethylase involved in IRF-4 expression, is reportedly induced by TLR stimulation (33). In our study, polyI:C stimulation increased Jmjd3 mRNA in F4/80$^+$ cells